CHARACTERIZATION AND APPLICATION OF MONOCLONAL ANTIBODIES AGAINST PORCINE EPIDEMIC DIARRHEA VIRUS

by

YIN WANG

B.S., Yangzhou University, 2010
M.S., Yangzhou University, 2013

A THESIS

submitted in partial fulfillment of the requirements for the degree

MASTER OF SCIENCE

Department of Diagnostic Medicine and Pathobiology
College of Veterinary Medicine

KANSAS STATE UNIVERSITY
Manhattan, Kansas

2015

Approved by:

Major Professor
Weiping Zhang

Copyright

Abstract

Porcine epidemic diarrhea virus (PEDV) causes acute diarrhea to pigs at all ages, resulting in high mortality rate of 80-100% in piglets less than one week old. Within one year after the outbreak in April 2013, PEDV has rapidly spread in the US and causes the loss of over 10% of the US pig population. Monoclonal antibody (mAb) is a key reagent for rapid diagnosis of PEDV infection. In this study, we produced a panel of mAbs against nonstructural protein 8 (nsp8), spike(S) protein, and nucleocapsid (N) protein of PEDV. Four mAbs were selected, which can be used in various diagnostic assays, including indirect immunofluorescence assay (IFA), enzyme-linked immunoabsorbent assay (ELISA), Western Blot, immunoprecipitation (IP), immunohistochemistry (IHC) test and fluorescence in situ hybridization (FISH). The mAb 51-79 recognizes amino acid (aa) 33-60 of nsp8, mAb 70-100 recognizes aa1371-1377 of S2 protein, and mAb 66-155 recognizes aa 241-360 of N protein, while mAb 13-519 is conformational. Using the mAb70-100, the immunoprecipitated S2 fragment was examined by protein N-terminal sequencing, and cleavage sites between S1 and S2 was identified. In addition, this panel of mAbs was further applied to determine the infection site of PEDV in the pig intestine. IHC test result showed that PEDV mainly located at the mid jejunum, distal jejunum and ileum. Results from this study demonstrated that this panel of mAbs provides a useful tool for PEDV diagnostics and pathogenesis studies.

Table of Contents

List of Figures

List of Tables

Acknowledgements

I would first like to appreciate my major supervisor, Dr. Weiping Zhang, for accepting me into his laboratory. Under his mentorship during the two years, I've acquired not only the knowledge, but the attitude to the science.

I would like to specifically acknowledge Dr. Ying Fang, for teaching me the experimental skills and helping to open my vision. I'm deeply influenced by her enthusiasm and ambition to the research.

I'm very grateful to my committee members, Drs. T.G.Nagaraja, Derek A. Mosier and Bruce Schultz, for their guidance and suggestion to my program. I would like to thank Dr. M.M. Chengappa, Dr. Jamie Henningson, Jennifer Hill and other faculties and staffs for their kind favor in my research.

My sincere appreciation goes to all the lab members and friends for their kind help. This includes Qiangde Duan, Rahul Nandre, Xiaosai Ruan, Yanhua Li, Zhenhai Chen, Rui Guo, Pengcheng Shang, Russell Ransburgh and Fangfeng Yuan.

I would like to thank my parents, Laizhong Wang and Peizhen Wang, for always inspiring and believing in me. Also I'd like to thank my parents in law, Jianming Guo and Jufang Qin, for supporting and encouraging me in the two years. Finally, I would express my deepest gratitude to my husband, Rui Guo, for his never-ending patience and understanding.

List of abbreviations

PED	porcine epidemic disease
PEDV	porcine epidemic disease virus
TGEV	transmissible gastroenteritis virus
EM	electron microscopy
SARS-CoV	severe acute respiratory syndrome coronavirus
MHV	mouse hepatitis virus
ACE2	angiotensin converting enzyme 2
nsps	nonstructural proteins
ER	endoplasmic reticulum
polyA	polyadenosine
ORF	open reading frame
pp	polyprotein
S	spike
E	envelope
M	membrane
N	nucleocapsid
PLP1	protease--papain-like proteases
DUB	deubiquitinating
IFN	interferon
ADRP	ADP-ribose-1’-monophosphatase
DMV	double membrane vesicles
RVN	reticulovesicular network
HB	helix bundle
HCT	helix at the C-terminal
SPR	surface plasmon resonance
SAM	S-adenosyl methionine
RdRp	RNA dependent RNA polymerase
NendoU	nidoviral uridylate-specific

	endoribonuclease
RBD	receptor binding domain
HR	heptad repeat region
RNP	ribonucleoprotein
NTD	N-terminal domain
CTD	C-terminal domain
IDR	intrinsically disordered region
RTC	replication transcription complex
LKR	linker region
IRF	interferon regulatory factor
TBK	TANK binding kinase
APN	Aminopeptidase N
dpi	days post infection
ELISA	enzyme-linked immunosorbent assay
IF	immunofluorescence
IHC	immunohistochemistry
HE	hematoxylin and eosin
PRCV	porcine respiratory coronavirus
mAb	monoclonal antibody
MEM	Eagle’s minimum essential medium
FBS	fetal bovine serum
hpi	hours post infection
moi	multiplicity of infection
HRP	horseradish peroxidase
NC	nitrocellulose
PNDF	polyvinylidene difluoride
IACUC	Institutional Animal Care and Use Committee
IP	intraperitoneal
PCR	polymerase chain reaction
FITC	fluorescein isothiocyanate

TCID50	50% Tissue Culture Infective Dose
DAPI	4',6-diamidino-2-phenylindole
OD	optical density
FISH	fluorescence In situ hybridization
RTC	replication and transcription complex
TRS	transcriptional regulatory sequence
FCoV	feline coronavirus

Chapter 1 - Literature Review

1.1 Porcine epidemic diarrhea (PED) and the etiological agent

Porcine epidemic diarrhea is an emerging infectious disease caused by porcine epidemic diarrhea virus (PEDV). PEDV spreads rapidly in US swine farms and results in a mortality rate of 80-100% in neonatal pigs. PED virus is transmitted through the fecal-oral route. Clinical studies showed that PEDV can spread to all farrowing, breeding and gestation rooms in a farm within 24 h, and all piglets developed watery diarrhea, vomiting and dehydration within 24 h after birth (1).

PEDV has been previously associated with sporadic outbreaks in European and Asian swine producing countries, causing significant economic losses to swine producers. The disease was first recognized in swine farms in the United Kingdom in 1971(2), but the causative agent, PEDV, wasn't detected or isolated until a severe diarrhea outbreak in Belgium in 1978. Different from transmissible gastroenteritis virus (TGEV), another porcine coronavirus that leads to diarrhea, PEDV was isolated from the enteric content and was designated as CV777 strain (3). PEDV spread in European countries during 1980s-1990s, including UK, Belgium, the Czech Republic and other European swine-producing countries (3-5). In Asia, PED was first identified in Japan in 1982 (6). Subsequently, an outbreak of PED was observed in South Korea (7). In China, a massive PEDV outbreak appeared in 2010(8). By now, the virus has been isolated in other Asian countries including Vietnam and Thailand (9-11). Since April 2013, PED has rapidly spread in the USA, and the disease continues to spread throughout North America. It was reported that by April 2014, approximate 7 million (almost 10% of the domestic pig population) pigs died from this disease, resulting to an estimated net annual decreases of US economy about $900 million to $1.8 billion (12) .

PEDV belongs to order *Nidovirales*, family *Coronaviridae*, and genus *Alphacoronavirus*, which also include Human coronavirus 229E, Human coronavirus NL63 and other batcoronaviruses. PEDV is genetically more closely related to BtCoV/512/2005 than to transmissible gastroenteritis coronavirus (TGEV), speculating a hypothesis that PEDV is originated from bats (13). The PED virus particle is approximate 130 nm in diameter with the bouyant density of 1.18. Under the electron microscope (EM), the PEDV virion has the characteristic appearance of coronaviruses, a fringe of large protrusions on virus envelop. The virus is moderately stable at 50 ℃. At 4 ℃, the virus is comparatively stable between pH 5 - 9, whereas at 37 ℃, it is stable only at pH 6.5 - 7.5 (14).

Swine are the only known host of PED virus. Mice, on the contrary, are specifically demonstrated to be non-competent vectors(15) . A recent study testing different cell types for PEDV propagation *in vitro* demonstrated that PEDV can infect cell lines derived from pig (ST cells; PK-15), human (Huh-7; MRC-5), monkey (Vero CCL-81) and bat (Tb1-Lu) (13). The current circulating strains in North America were first isolated using Vero cell lines (Vero CCL-76 and Vero CCL-81) (16, 17).

PEDV has the similar life cycle as other coronaviruses, such as severe acute respiratory syndrome coronavirus (SARS-CoV) and mouse hepatitis virus (MHV). Coronaviruses are enveloped viruses that enter the host cells through the fusion of their S protein with host cell plasma membrane. The process begins with the binding of the S protein to host cellular receptors – human angiotensin converting enzyme 2 (ACE2) for SARS-CoV and Human coronavirus NL63, murine CEACAM1 for MHV, and porcine aminopeptidase N (CD13) for PEDV and TGEV, followed by the translocation of the virions into host cell cytoplasma through endocytosis. In the endosome, the fusion process between the viral envelope and the cell

membrane is activated by the homogenous or heterogenous proteases, leading to the release of the viral RNA genome into the cytoplasma. The replicase polyproteins 1a and 1ab are firstly synthesized and then cleaved into 15 or 16 nonstructural proteins (nsps) by viral proteinases, including nsp3 and nsp5. Secondly, the nsps participate in genome replication, involving synthesis of full-length negative-strand RNA at a low concentration which serves it as the template for full-length genomic RNA. Meanwhile, discontinuous RNA also is synthesized for transcription of multiple subgenomic mRNAs (18). All multiple subgenomic mRNAs share with an identical 3' end terminal and 5' leader sequence, considered as a hallmark of coronaviruses and other nidoviruses. Lastly, mRNAs afterward translate to viral structural proteins and some accessory proteins. After synthesized and posttranslational modified in the endoplasmic reticulum (ER) and Golgi compartment, mature structural proteins are assembled with genomic RNA into virus virions, which are released outside through exocytosis for the next generation infection (19).

1.2 PEDV genome organization and viral gene function in coronaviruses

PEDV has a single-stranded positive-sense RNA genome with the size of approximately 28 kilobases, with exclusion of the polyadenosine (polyA) tail. The US NPL strain shares the same genome organization with the prototype PEDV CV777 strain, characterized by a gene order of 5'- open reading frame 1a/1b (ORF1a/1b)-S-ORF3-E-M-N-3'. The ORF1a/1b which occupies approximately 2/3 of the virus genome at 5'- end encode the replicase pp1a and pp1ab, produced by − 1 ribosomal frameshift where the translation doesn't stop at the endpoint of ORF1a. The pp1a and pp1ab are further cleaved into 16 nonstructural proteins. The 1/3 3'- end genome includes 5 ORFs, encoding 4 structure proteins, namely, spike (S,150-220kDa),

envelope (E, 7kDa), membrane (M, 20-30kDa) and nucleocapsid (N, 58kDa) protein and an accessory protein (Figure 1) (69).

1.2.1 Coronavirus nonstructural proteins

The coronavirus nsps, generated from the proteolytic cleavage of pp1a and pp1ab by the viral protease--chymotrypsin-like protease 3CLpro (also called main protease or Mpro) and protease--papain-like proteases (PLP), play an important role in the viral replication and transcription (18).

Nsp1: nsp1 only exists in alpha and beta coronavirus genus. It is the first N-terminal protein released from the ORF1a polyprotein pp1a, cleaved by nsp3 (PLpro domain) (20). The sequence and structure of nsp1 between different genera share low homogeneity. TGEV nsp1 is a protein of 9 kDa, whereas nsp1 of SARS-CoV is of 28 kDa. Differed from the structure of TGEV nsp1 which is characterized by an irregular six-stranded β-barrel with an-α-helix, the SARS nsp1 includes a globular domain and some disordered regions (21, 22). However, nsp1 of the two genera share similar function, as they can functionally suppress the innate immune response and the expression of host mRNA (23, 24).

Nsp2: nsp2 is also cleaved from pp1a the protease activity of nsp3 (PLpro domain). The exact function of nsp2, however, remains unclear. The MHV and SARS-CoV with nsp2 deletion could survive in the cell culture, suggesting nsp2 is dispensable for viral replication (25). It was found that the nsp2 deletion attenuates viral growth and RNA synthesis; compared to the wild type strains, the nsp2 deletion strains showed a lower virus titer and RNA defect (25).

Nsp3: nsp3 carries one or two papain-like proteases which belong to the cysteine protease family (26). The nsp3 subunits of alpha coronaviruses and subgroup 2a beta coronaviruses contain two active Papain like protease (PL^{pro}) domains-- $PL1^{pro}$ and $PL2^{pro}$. That differs from

SARS-CoV, a 2b beta coronaviruse which contains only $PL2^{pro}$. The PL^{pro} protein processes the cleavages between nsp1 | nsp2, nsp2 | nsp3, and nsp3 | nsp4 sites of the coronavirus (26, 27). In addition, the $PL2^{pro}$ domain of SARS-CoV and HCoV-NL63 has deubiquitinating (DUB) activity, and antagonizes induction of type I interferon (IFN) (28). The nsp3 also contains domains with ADP-ribose-1"-monophosphatase (ADRP) activity and single strand RNA binding ability (29, 30).

Nsp4: Data from studies on mutants showed that coronavirus nsp4 is critical in double membrane vesicles (DMV) biogenesis since infection of the temperature sensitive phenotype MHV with nsp4-N258T resulted in dramatic reduction of DMVs (31).

Nsp5: nsp5 is the main protease of coronavirus or 3C-like protease (M^{pro}, $3CL^{pro}$), and is responsible for processing 11 cleavage sites from nsp4 to nsp16 (26). Nsp5 is essential for virus replication (26). It was demonstrated that disruption of the cleavage sites at nsp6-nsp7, nsp7-nsp8, nsp8-nsp9, and nsp10-nsp11 were lethal for viral propagation (32).

Nsp6: Coronavirus nsp6, together with nsp3 and nsp4, are membrane anchor proteins; they contain transmembrane domains. Those proteins are believed to participate in formation of reticulovesicular network (RVN) and DVM (33).

Nsp7-8: nsp7 and nsp8 form a hollow cylinder like complex on the surface of inner channel for binding to the double stranded RNA and initiating the de novo RNA synthesis. The structure of nsp7 is featured with 3 α-helix bundles (HB) at the N-terminal, HB1, HB2 and HB3, and one α- helix at the C-terminal (HCT). The nsp8 has two different conformations—nsp8I and nsp8II. Both have “golf-club like structure”, of which N terminal is the shaft comprised of α-helix, while the C terminal is the head including 3 α- helices and 7 β-strands. The difference between type I and II mainly is the shaft part. Two short helices, NH1 and NH2, and one very

long helix domain, NH3, form into the type I shaft. In type II, only NH3 exists, with two parts, NH3α and NH3β. Eight copies of nsp7 cross link with four copies of nsp8I and 4 copies of nsp8 II respectively to form the hexadecamer (34, 35).

Nsp9: the SARS-CoV nsp9 has been demonstrated to have RNA and DNA binding activity in surface plasmon resonance (SPR) and fluorescence experiments. Two copies of nsp9, each with 7 β-strands and a single α-helix for a monomer, form a dimer through the interaction between the helices (36). The single amino acid mutations of G100E and G104E are lethal to the virus indicating that the $_{100}$GXXXG_{104} motif in the dimer is critical for viral replication (37).

Nsp10, nsp14 & nsp16: the interaction between nsp10 and nsp14 or nsp16 has a remarkable inference on the fidelity and methylation of the virus (38). The nsp10 is the activator of nsp14 and nsp16. To be functionally, 12 copies of nsp10 monomers assemble into the spherical dodecameric architecture (39). The nsp14 has two domains: S-adenosyl methionine (SAM)-dependent (guanine-N7) methyltransferase (N7-MTase) at the C-terminal and 3’ to 5’ exonuclease (ExoN) at N-terminal. The nsp16 acts as the AdoMet-dependent (nucleoside-2’O)-methyltransferase (2’O-MTase) (38).

The N7-MTase of nsp14 and 2'-O-MTase of nsp16 are involved in the RNA methylation and capping-1 formation. They are spectulaed catalyze the transfer of the methyl group from the methyl donor SAM or AdoMet to RNA substrate (40, 41). The nsp14 ExoN plays a role to greatly increase of replication fidelity for MHV. Studies of mutants indicated that replacement of the conserved ExoN active-site residues with alanines (D89A, E91A, D272A and R277A) resulted in 15-fold decrease of viable growth and RNA synthesis, compared to wild-type virus (42).

Nsp11: while the function of nsp11 is still not clear, the proteolytic processing at the cleavage sites between nsp10–nsp11/12 of MHV and IBV was demonstrated essential for the viral replication (43).

Nsp12: nsp12 is the viral RNA dependent RNA polymerase (RDRP) with canonical RDRP motifs locating at the C-terminal. Nsp12 initiates the RNA extension with help from a primer, which comes from the *de novo* synthesis of nsp8 in coronavirus. However, the nsp12 shows 20-fold stronger polymerase activity of RdRp than the complex of nsp7 and nsp8 (35, 44).

Nsp13: nsp13 is a helicase of the virus, which unwinds both RNA and DNA in a 5'-to-3' direction. It is also a NTPase with ability to hydrolyze nucleotides and ribonucleotides. In addition, nsp13 has RNA 5'-triphosphatase activity related to the viral capping process (45).

Nsp15: nsp15 is a viral endoribonuclease, of which C-terminal region contains a nidovirus-specific motif known as nidoviral uridylate-specific endoribonuclease (NendoU). It was revealed that the Mn^{2-}-dependent endoribonuclease acts with the preference to the cleavage of double-stranded RNA substrates upstream and downstream of uridylates in GU or GUU sequences (45) (Ivanov KA, 2004b).

1.2.2 Coronavirus structural proteins

The structural proteins spike protein(S), envelop protein (E), membrane proten(M) and nucleocapsid protein(N) translated from multiple subgenomic mRNAs contribute to the virus particle architecture.

Spike protein(S): Coronavirus has the typical structure of a crown-like corona. Coronavirus S protein, in a form of trimers, and displayed on the surface of the virus membrane, like a corona. Like the glycoprotein of Ebola virus, S protein is classified as class I viral fusion proteins or type I transmembrane protein. During infection, the spike protein is cleaved into S1

and S2 subunits by the protease, including trypsin and cathepsin (46). This cleavage is thought to be essential for initiation of cell-to-cell fusion and virus entry into cells. The S1 bears the receptor binding domain (RBD), thus is responsible for receptor binding. S1 subunit is the determinant for virus-receptor interaction, host range, and virus cell and tissue tropism (47). S2 subunit bears fusion peptide, heptad repeat region 1 (HR1) and HR2, which serve as important components for virus-host fusion and syncytial formation. Further, it was demonstrated that S protein from most coronaviruses, including SARS-CoV, MHV and PEDV, is able to be cleaved by trypsin at two distinct sites. One cleavage site is located at the boundary of S1 and S2, named S1/S2 site. The other, named S2', located at very adjacent to the fusion peptide. The S2' is believed to be crucial for fusion activity of the S protein (48-50).

Nucleocapsid protein (N): N protein is the most abundant protein in the virus infecting cells. N protein packs the viral genome RNA molecule into a ribonucleoprotein (RNP) complex, constituting the essential template for replication by the RDRP complex (51). N protein contains a N-terminal domain (NTD), a C-terminal domain (CTD), and intrinsically disordered regions (IDRs). Multiple sites within the three regions are able to bind and activate with RNA (52-54). Besides binding to genome RNA, N protein has been demonstrated to associate with the replication transcription complex (RTC); for example, the N protein of MHV binds to the viral nsp3 through the NTD and the linker region (LKR) (55). Also, N protein of SARS-CoV was demonstrated to inhibit the synthesis of interferon-β (56). Recently, PEDV N protein was shown to antagonize IFN-β production by sequestering interaction between interferon regulatory factor 3 (IRF3) and TANK binding kinase 1(TBK1), a critical step in type I IFN signaling (57).

Membrane protein (M) and Envelop protein (E): The M protein is the most abundant in the viral envelope, while the E protein is less abundant. Both proteins have been demonstrated to

be essential for virus assembly (58). Previously, it showed that M protein together with another M protein as the dimer interacts with E protein, S protein and N protein (58, 59).

1.2.3 Coronavirus replication/transcription complex (RTC)

The coronavirus replication/transcription complex (RTC) is composed of all non-structural proteins (nsp1-15 or nsp16). The RTC is associated with cytoplasmic membranes, the double membrane vesicles (DMVs), mostly believed that derived from endoplasmic reticulum (ER). Among the non-structural proteins of SARS-CoV, nsp3, 4 and 6 can induce the DMV formation and help RTC anchor to the membrane. DMVs are ideal place for RNA replication for the comparative high concentrated components, and also provide the protection from host defense mechanism that could be trigged by dsRNA intermediates during the replication (60, 61).

1.3 Pathogenesis

PEDV infects pigs of all age, with suckling pigs are often of the most severely affected. Clinical signs are often resolved within 7–10 days post infection (dpi) (62). Aminopeptidase N (APN), which abundantly presents at the porcine small intestinal enterocytes, is considered the receptor for PEDV infection, (13, 63). PEDV can attach to the enterocytes and infect pigs rapidly, contributing to villous atrophy in the small intestines. A majority of susceptible enterocytes are destroyed likely around 6 or 7 dpi, resulting from higher viral shedding in infected pigs (64). The acute watery diarrhea induced by PEDV is the consequence of malabsorption of small intestinal enterocytes. Pig small intestinal enterocytes are the primary site to process and absorb water and nutrients including ion, sugar, peptide, lipid, and vitamin, and also the major barrier against enteric pathogens (65). A loss of electron density of the cellular cytoplasm and rapid degeneration of mitochondria, due to virus replication inside

enterocytes, result in a lack of transport energy needed for absorption, leading to cell dysfunction (66). Additionally, PEDV infect goblet cells; a decrease of goblet cells increases the risk of pathogen infection (67).

1.4 Diagnostics

Several molecular biological and immunological techniques have been developed to specifically diagnose PEDV. These includes PCR, real-time PCR, enzyme-linked immunosorbent assays (ELISA), immunofluorescence (IF) tests, immunohistochemistry (IHC), and electron microscopy (EM). The PEDV strain circulating in the US was first isolated by the Iowa State University Veterinary Diagnostic Laboratory (ISUVDL) on April 2013. Because of clinical symptoms that are consistent to of TGE, tissue samples from small intestines were collected and stained with hematoxylin and eosin (H&E) for microscopic examination. Histology revealed severe atrophy of villi in all segments of the small intestines with occasional villus-epithelial syncytial cells. Therefore, it was concluded that a pathogen causes damage of the small intestine. Afterwards examination of feces and/or intestinal contents with nested real-time PCR revealed positive amplification of the S gene and the N gene of PEDV, but negative of TGEV and Porcine respiratory coronavirus (PRCV). Further sequence comparison showed high identity to known PEDV strains. Additionally, negative-staining EM suggested presence of coronavirus-like particles in the feces and/or intestinal contents. Lastly, a mAb specific to PEDV N protein recognized abundant viral nucleocapsid proteins in the cytoplasm of epithelial cells from IHC assay. Together, results from these studies concluded the causative agent is PEDV (68).

1.5 Purpose of this research

PEDV causes acute diarrhea to pigs at all ages, resulting in high mortality in piglets less than one week old. Since April 2013, PEDV has rapidly spread in the US and causes the loss of

over 10% of the US pig population. Therefore, PEDV prevention is essential for the pork producers in US. Disease diagnosis or recognition is the first step to determine the etiology, which is foundation of disease control and prevention. Currently, different kinds of immunological techniques have been applied into disease diagnosis, including IFA, IHC and ELISA. In most of the methods, monoclonal antibody (mAb) is the key reagent to recognize antigens directly. In this study, we will screen the PEDV viral proteins to find the most antigenic ones, and used them to develop monoclonal antibody production. The mAbs produced in this study will provide a useful tool for PEDV diagnostics and potentially pathogenesis studies.

Figure 1. Schematic diagram of PEDV genome and virion(69)

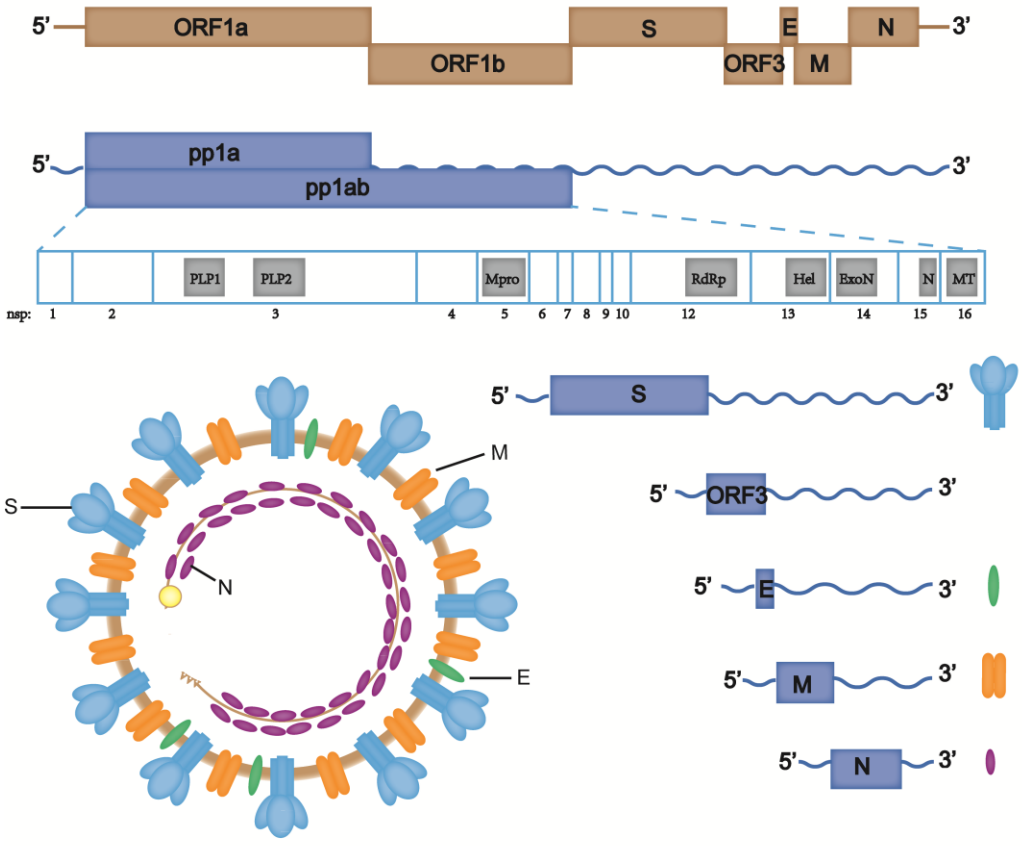

Modified from Song, et al, 2012

Chapter 2 - Materials and methods

2.1 Cells and virus

Vero76 (ATCC, CRL-1587 ™) and HEK-293T cells used in this study were cultured in Eagle's minimum essential medium (MEM) (Invitrogen; Waltham, MA) containing 10% fetal bovine serum (FBS) (Sigma; St. Louis, MO), 1% Penicillin-Streptomycin (Gibco; Waltham, MA), and 0.25ug/ml Fungizone® Antimycotic (Gibco). PEDV strain KS1309 (GenBank Accession: KJ184549.1) was propagated in Vero76 cells. Vero76 cells were infected with the virus in the infection MEM medium with 2% Trptose Phosphate Broth solution (Sigma), 1ug/ml L-1-Tosylamide-2-phenylethyl chloromethyl ketone (TPCK) (Sigma).

2.2 Virus concentration and titration

To propagate PEDV KS1309, Vero76 cells were infected with the virus at moi of 0.01 and the supernatant was collected at 18 hours post infection (hpi). Macrosep Advance Centrifugal Device (PALL; Port Washington, NY) was sterilized with 70% ethanol for 20 minutes in the biological safety cabinet, filtered and washed with the DNase/RNase-free distilled water (Invitrogen) for 3 times. Fifty ml of virus infected cell culture supernatant was added into the device and was centrifuged at 3,000×g for 1 hour at 4℃. The cell culture medium was then replaced with PBS by three additional wash with PBS. The concentrated virus in approximately 1ml PBS were gently resuspended, pooled, and stored at -80℃ freezer. For the virus titration, the confluent Vero76 cells in the 96-well cell culture plates were infected with the PEDV of ten-fold serial dilutions (10^{-1} ~ 10^{-7}) in octuplicate. Cells were incubated in a CO_2 incubator at 37^0C with 5.0% CO_2. After 3 hour incubation, the virus infected cell culture supernatant was replaced with fresh

infection medium. At 18-hpi, cells were fixed with acetone and methanol mixture at the ratio of 3:2 for 30 min at 4^0C. The cells were immunostained with the rabbit polyclonal antibody (pAb; 1:500) (Genscript, Piscataway, NJ) against PEDV M protein. After washing with PBS for 3 times, FITC conjugated goat-anti-rabbit IgG pAb (Jacksonimmuno; West Grove, PA) was added as the secondary antibody. Finally, the virus titer was determined by the fluorescence analysis and calculated as described previously (50).

2.3 Cloning of DNA fragments coding PEDV nonstructural and structural proteins

Nucleotide fragments coding the nsp1, truncated nsp2 (445-711aa), nsp3 (PLP1 domain), nsp5, nsp7, nsp8, nsp9, nsp10, S1, S2, N, M, and E of PEDV strain KS1309 were cloned for recombinant proteins to be used as coating antigens for ELISA and immunogens for antibody production. These cDNA fragments were generated in RT-PCR using SuperScript® III One-Step RT-PCR System with Platinum® Taq DNA polymerase kit (Invitrogen) by following the manufacturer's protocol. Briefly, 25 µl 2X Reaction Mix (a buffer containing 0.4 mM of each dNTP, 2.4 mM MgSO4), 1 µg template RNA extracted by QIAamp Viral RNA Mini Kit (Qiagen), 1 µl Anti-sense primer (10 µM), 2 µl High Fidelity Enzyme Mix, in a final volume of 50 µl (with autoclaved distilled water) were premixed in 0.2-ml, nuclease-free, thin-walled PCR tubes on ice. The one-step RT-PCR program consists of 1 cycle 55˚C for 30 min, 1 cycle 94˚C for 2 min, 40 cycles (94˚C for 20s, 53˚C for 30s, 68˚C for 1 min), 1 cycle 68˚C for 10 min, and hold at 4˚C. RT-PCR products were gel purified with a QIAquick gel extraction kit (QIAGEN). Purified RT-PCR products were double digested by restriction enzymes *Bam*HI and *Not*I (NEB;

Ipswich, MA) and then ligated into pET28α (+) vector (Novagen; Madison, WI) with T4 ligase (NEB; Ipswich, MA). Ligated product was used to transform *Escherichia coli* (*E.coli*) DH5α cells (Invitrogen). Transformed *E. coli* bacteria selected with Kanamycin were further verified with enzyme restriction digestion and DNA sequencing.

2.4 Protein expression and purification

The recombinant proteins, PEDV nsp1, truncated nsp2 (445-711aa), nsp3 (PLP1 domain), nsp5, nsp7, nsp8, nsp9, nsp10, S1, S2, N, M, and E, were expressed andextracted as described previously(70) . In brief, plasmids carrying the gene coding each protein were introduced into competent *E.coli* BL21 (DE3) cells (Novagen). After sequencing verification, each transformat was cultured in LB (BD Diagnostic Systems; San Jose, CA) containing kanamycin (30ug/ml) at 37^0C overnight. One ml overnight grown bacteria culture was inoculated into 50 ml 2×YT medium containing kanamycin (30ug/ml) (BD Diagnostic Systems, incubated to the OD reading to 0.4~0.6. Bacteria were induced by 1.0 mM isopropyl-1-thio-beta-D-galactopyranoside (IPTG) (Sigma), and continuously cultured for additional 4 h at 37^0C. Total proteins were extracted with B-PER Bacterial Protein Extraction Reagent (Life technologies; Carlsbad, CA) by following the manufacture's protocol. Briefly, the bacterial overnight grown was centrifuged at 5000 × g for 10 minutes. Bacterial pellets, after frozen and thawed at least once, were suspended with 5mL of B-PER Reagent and 5ug/ml lysozyme (Life Technologies) was pipetting up and down. Bacterial suspensions were incubated for 15 minutes at room temperature. The lysates were separated into soluble proteins in the supernatant and insoluble protein in the pellets by centrifugation at 15,000 × g, for 15 minutes at 4^0C. Protein samples were examined with SDS-PAGE to determine whether

the recombinant proteins were came from the pellets. To extract recombinant protein, the Ni–NTA agarose (QIAgen) affinity-isolation procedure was performed by the following the manufacturer's protocol. Briefly, 1 ml of the 50% Ni-NTA slurry was mixed with 4 ml bacterial lysate and gently shaken overnight at 4^0C. 0.5 ml of each buffer B (100 mM NaH_2PO_4, 10 mM Tris Cl, 8 M urea, pH 8.0), buffer C (100 mM NaH_2PO_4, 10 mM Tris•Cl, 8 M urea, pH 6.3), buffer D (100 mM NaH_2PO_4, 10 mM Tris•Cl, 8 M urea, pH5.9), and buffer E (100 mM NaH_2PO_4, 10 mM Tris•Cl, 8 M urea, pH4.5) was used to wash and elute the protein for 3 times respectively. Wash fraction were collected for the SDS-PAGE. To further purify the protein, the band of interest visualized with staining of 0.25M KCl was cut from the SDS-PAGE, and protein was eluted with the protein elution buffer (25mM Tris base, 192mM Glycine, and 0.1% SDS) using the Model 422 Electro-Eluter (Bio-Rad; Hercules, CA). After 4h in the ice-water bath, eluted proteins were condensed by centrifuge with Amicon Ultra-4 Centrifugal Filter Units (Millipore; Darmstadt, Germany).

2.5 Enzyme-linked immunosorbent assay (ELISA)

2HB plates (Thermo Fisher; Waltham, MA) were coated with purified proteins (100 ng/ well) in antigen coating buffer (15 mM Na_2CO_3, 35 mM $NaHCO_3$, pH9.6). Coated plates (Thermo Fisher) were incubated at 37^0C for 1h and then at 4^0C overnight. The plates were blocked with 10% non-fat milk with incubating at 37^0C for 1h and washed 3 times with PBST (0.05% Tween 20 in PBS). PEDV positive serum diluted by 1:50 utilized as the primary antibody was added to each well; plates were incubated at 37^0C for 1h and washed 3 times with PBST. Horseradish peroxidase (HRP)-conjugated goat anti-swine IgG (heavy + light chains) (1:5000; KPL, Gaithersburg, MD) was used as the secondary

antibody. Plates were incubated at 37^0C for 1 h, and washed 3 times with PBST. After adding peroxidase TMB substrate and substrate Solution B (1:1, KPL), plates were stored in the dark at room temperature for 30min and read the ODs using SpectraMax 190 Microplate Reader at a wavelength of 650 (Molecular Devices, Sunnyvale, CA).

2.6 SDS-PAGE and Western-blot assay

Protein samples in protein loading buffer were boiled for 10min and examined in the SAS-PAGE. Electrophoresed proteins in the SDS-PAGE were transferred to a nitrocellulose (NC, for western-blot assay; GE, Marlborough, MA) or Polyvinylidene difluoride (PVDF, for protein sequence; Invitrogen, Carlsbad, CA) membrane which was pretreated with methanol by soaking for 5 min. Transfer was completed at 70 voltages for 3h 40min, using the trans-blot system (Bio-Rad). After blocked with 10% non-fat milk for 2h, at room temperature, the membrane blot was incubated with mAbs (13-519, 70-100, 66-155 and 51-79) as the primary antibody for 1 h at 37^0C, and was washed 3 times with PBST. Then, washed membrane blot was incubated with donkey-anti-mouse IRDye® 800CW Secondary Antibody (1:5000; Li-Cor; Lincoln, NE) for 1 h at 37^0C. After 3 washes with PBST, the membrane was examined by Odyssey® Fc Dual-Mode Imaging System (Li-Cor).

2.7 Mouse immunization and monoclonal antibody production

Mouse immunizations were conducted by complying with the protocol proved by the Institutional Animal Care and Use Committee (IACUC). Twelve 8-week-old BALb/C female mice were separated, into 4 groups (3 mice per group), were immunized with antigens mixed with equivalent volume of Freund's incomplete adjuvant. Based on the Western-blot and ELISA results, proteins with high antigenicity for the 3 groups were

purified N protein, a mixture of S1 and S2 proteins, a mixture of Nsp7 and Nsp8, respectively, 50ug/mouse. The other group mice were immunized with purified PEDV, 10^7 TCID50/mouse. IP immunizations were carried out 3 times, at an interval of 2 weeks. The splenocytes of the immunized mice were fused with NS-1 myeloma cells. Specific anti-PEDV mAbs were screened by ELISA and indirect IFA as described previously (71). The mAbs were concentrated by both ways of ascites production in retired mice and sediment with saturated ammonium sulphate solution (Thermo Fisher) from the cell supernatant. Briefly, the pristine (Sigma) primed retired mice were injected with hybridomas (5×104 cells per mouse) producing the mAbs specific for PEDV protein through IP. The mouse ascites fluids containing the mAbs were collected after 10 days after the injection. The saturated ammonium sulphate solution sediment was conducted followed by the manufacturer's protocol.

2.8 Antibody epitope mapping

Indirect immunofluorescence assay (IFA) was used to determine the epitopes which were recognized by mAbs specific to PEDV S, N, or nsp8 protein. The full length cDNA or truncated cDNA fragments of PEDV S, N or nsp8 were cloned into the expression vector pEGFP-N (Clone Tech; Mountain View, CA). HEK-293T cells were transiently transfected with recombinant vectors and the GFP tagged peptides were expressed. The cells were fixed, then immunostained with the mAbs (1:1000) as the primary antibody and the CAL594 conjugated anti-mouse IgG (1:500) as secondary antibody, and observed under EVOS® Imaging Systems (Invitrogen).

2.9 Antibody isotype determination

Isotypes of the mAbs were determined by the IsoStrip Mouse Monoclonal Antibody Isotyping Kit (Sigma) by following the manufacturer's protocol. Briefly, the ascites samples or the hybridoma supernatant were diluted by 1:10,000 or 1,000 respectively with 1% BSA/ PBS. The strips were soaked with the samples for 1-5 min when the blue bands appeared above the letters in one of the class or subclass windows as well as in either the kappa or lambda window, indicating the heavey and light-chain composition of the mAbs.

2.10 Immunoprecipitation and Western-blot

Vero 76 cells were infected with KS1309 PEDV strain at 0.1 MOI. At 18 hpi, cells were lysed using immunoprecipitation lysis buffer as described in manual (Pierce). The cell lysates clarified by centrifuging at 4℃ immunoprecipitated with appropriate antibodies and bound into protein A/G magnetic beads (Pierce) at 4℃ overnight. The immunoprecipitation products were separated by SDS-PAGE using 8-16% Tris-Glycine gradient gel (Invitrogen). The recombinant proteins were also used for SDS-PAGE and transfer onto NC membrane (GE) as the steps described above. The membrane was immunostained by the mAbs or hyper-immune swine serum. IRDye® 800CW conjugated donkey-anti-mouse IgG (1:5000) was used as secondary antibody (Li-cor). The membranes were examined by Odyssey® Fc Dual-Mode Imaging System (Li-cor).

2.11 Fluorescence in situ hybridization (FISH) and indirect fluorescence assay (IFA)

Stellaris® FISH Probes were designed against the RNA coding region of nucleocapsid protein of PEDV by utilizing the Stellaris® RNA FISH Probe Designer (Biosearch

Technologies, Petaluma, CA). Fixed Vero 76 cells were hybridized with the RNA of PEDV N gene Stellaris RNA FISH Probe set labeled with CAL594 (Biosearch Technologies, Inc.), by following the manufacturer's instructions. Briefly, Vero76 cells were infected with PEDV at moi of 0.1 in 35mm glass bottom dishes (MatTek; Ashland, MA) and fixed at 6, 9, 12, 18 hpi with the fixation buffer (3.7% Formaldehyde solution in nuclease free PBS) and permeabilized with 70% ethanol for at least 1 hour at 4 ℃. After discarding the ethanol, wash buffer A (20%Stellaris RNA FISH Wash Buffer A and 1% Deionized Formamide in nuclease-free water) was added and incubated for 5 min at room temperature. Within the humidified chamber, dispense 100 μl of the Hybridization Buffer containing probe plus appropriately diluted primary antibody onto the cells following by 4 hours incubation in the dark at 37 ℃. After removing the Hybridization Buffer gently, 1 mL of wash buffer A and goat-anti-mouse pAb conjugated with Alexa 488 (1:500; Jacksonimmuno, West Grove, PA) were added as the secondary antibody. For another 1 hour incubation at 37℃ in the dark, the nuclei were counterstained with 1ug/ml 4',6-diamidino-2-phenylindole (DAPI, Invitrogen). Then, the cells were washed with wash buffer B, and the cover slips were removed by the bottom glass removal fluid (MatTek, Ashland, MA). Finally, the cells were mounted with Prolong® Gold anti-fade reagent (Invitrogen) and observed under the confocal microscopy LSM 880 (Zeiss; Pleasanton, CA).

2.12 Immunohistochemistry (IHC) assay

The pigs were infected with PEDV positive grounded porcine intestine. At the 5 dpi, tissues were collected, included spleen, lung, tonsil, stomach, mesenteric lymph nodes, duodenum, proximal jejunum, mid jejunum, distal jejunum, cecum, ileum and colon, and

fixed in 10% neutral buffered formalin (sigma) at room temperature. After trimming into 1-niche-thick, the tissues in the cassettes were processed using a Tissue-Tek VIP automatic tissue processor (Sakura, Finland) with the routine overnight run and embedded into paraffin wax (Tissue-Tek). Embedded blocks were placed on the ice for a short time, and cutted into 4 μm sections. Sections were floated onto a warm (42℃) water bath, and were picked up onto Superfrost plus microscope slides (Fisherbrand).

Slides were positioned at a vertical rack for air dry overnight, placed in the warmer at 55℃ for 25 min, and dewaxed for 15 min. Detailed steps included: three times in the mixture of XS-3(Statlab) and xylene (Fisher Scientific) for 5 min, twice in 100% ethanol (Fisher Scientific) for 2 min, once in 95% ethanol for 2 min, and once in 80% ethanol in 2 min. Next, the slides were steamed in the citrate buffer for 30 min for antigen retrieval, cooled down on the bench for 20min and cleaned in the water holder for 5min. The tissues were further edged by the ImmEdge pen (Vector Laboratories, Burlingame, CA), blocked with the protein block (Dako, Carpinteria, CA) for 10min at 37℃, incubated with 1:200 diluted mAbs (13-519, 70-100, 66-155 and 51-79) as the primary antibodies at 37℃ for 1h, and ALEXA 488 conjugated goat-anti-mouse pAb (1:500; abcam, Cambridge, MA) as the secondary antibody at 37℃ for 1h. After 3 × 5 minute washes in PBS, the tissue samples were counterstained with ActinRed™ 555 ReadyProbes® Reagent (life technologies) for 30min at 37℃ and DAPI for 10min at room temperature. Followed by mounting with Fisherfinest™ Premium Cover Glasses (Fisher scientific) by ProLong® Gold antifade reagent (Invitrogen), the slides were air dried overnight and visualized with the LSM 700 confocal scanning microscope (Zeiss).

Chapter 3-Results

1. Antigen production

RT-PCR products of full-length or fragments of nsp1, nsp2, nsp3, nsp5, nsp7, nsp8, nsp9, nsp10, S, M and N from PEDV KS1309 strain were cloned into pET28α and expressed in BL21 (DE3). All proteins were expressed at high levels and purified in the insoluble form. Proteins were purified for an additional electro-eluting method and were refolded. Purity of the recombinant proteins was evaluated in SDS-PAGE and Coomassie blue staining. As shown in Figure 3.1.1, all the His-tagged recombinant proteins were at their expected sizes list here. Each protein was shown antigenic confirmed from Western blot analysis and indirect ELISA assay with the PEDV positive porcine serum standard (Figure 3.1.2). Nsp2, nsp7, nsp8, nsp9, S1, S2, M and N were recognized by pig anti-PEDV sera. Based on the OD values of indirect ELISA assay, N, Nsp7, M, S1 and S2 strongly interact with pig immune sera (OD value>0.7), nsp8 and nsp9 also interact with pig immune sera (0.4<OD value<0.7) (Figure 3.2). Results of indirect ELISA were found consistent with those of Western-blot assay.

2. Production and isotype detection of monoclonal antibodies against PEDV

Based on the results of Western-blot and indirect ELISA, N, mixture of S1 and S2, mixture of Nsp8 and Nsp9 and purified PEDV were selected for mouse immunization. Hybridoma clonies generated from the cell fusion were screened by indirect IFA. After the subcloning, the hybridomas producing mAb against PEDV N protein was identified, named as 66-155. In the PEDV immunization group, hybridomas producing mAbs against PEDV S protein was identified, named as 13-519. In the S1 and S2 mixture immunization group, hybridomas producing mAb against PEDV S2 protein was identified, named as 70-100. From the nsp7 and nsp8 mixture immunization group, hybridomas producing mAb against PEDV nsp8 was

identified, named as 51-79. Isotypes of monoclonal antibodies were detected by IsoStrip Mouse Monoclonal Antibody Isotyping Kit (Roche, Indianapolis, IN), except 13-519 which belongs to IgG2a, 70-100, 51-79 and 66-155 are IgG1 (Table 3.1).

3. Epitope mapping

Epitopes recognized by the anti-S, anti-N and anti-nsp8 mAbs was determined by immunofluorescence assay. HEK-293T cells were transiently transfected with DNA encoding different S protein peptides (S1-1386, S1131-1386, S1260-1386, S1358-1386, S1371-1377), N protein peptides (1-441, 241-441, 361-441), or nsp8 peptides (S1-140, S1-60, S1-33) expressed in the vector of pEGFP-N1 (Figure 3.3). MAb 13-309 could only recognize the full-length S protein which indicates that it may interact with a conformational epitope. MAb 70-100 could recognize seven amino acids (GPRLQPY) at the C-terminal of S2 protein which has been reported as a neutralizing epitope (72). MAb 66-155 could recognize fragment (1- 441), (241-441), but not (361-441), indicating this antibody recognize an epitope within 241-360 amino acids of N protein. MAb 51-79 could recognize fragment (1-140), (1-60), but not (1-33), indicating this antibody recognize an epitope within amino acids 33-60 of nsp8 protein.

4. Immunoprecipitation and Westernblot assay

To investigate the interaction between the proteins and the antibodies, mAbs were subjected to pull down the viral proteins from the PEDV infecting Vero76 cell lysates. The SDS-PAGE result shows mAbs 13-519 and 70-100 could pull down S and S2 protein, respectively while mAbs 66-155 and 51-79 could not pull down the viral proteins from the cell lysate (Figure 3.4.1 A). Western-blot result has confirmed the SDS-PAGE result (Figure 3.4.1 B). MAb 70-100 was subjected to detect S protein pulled down by mAb 13-519 due to the 13-519 could not recognize the S in Wetern-blot. S2 protein pulled down by mAb 70-100 could also be detected

by porcine anti-PEDV serum. In this study, the recombinant proteins expressed in *E.coli* were used as control. Except mAb 13-519, mAbs 70-100, 66-155 and 51-79 could detect the recombinant protein. Interestingly, besides the expected S2 protein band above 50kDa, another protein band was pulled down by mAb 70-100 between 37-50KD (Figure 3.4.2). Based on the result of N-terminal sequence, the second cleavage site S2' in S2 protein was identified.

5. Intracellular co-localization of S, N and Nsp8 with viral genomic RNA

In order to evaluate characteristic of the mAbs in IFA and to determine the correlation between the viral protein and viral genomic RNA, we performed RNA-FISH and immunofluorescence assay. The PEDV-infected cells were fixed every 3 hours from 6 hpi to 18 hpi, hybridized with 48 CAL 594 conjugated DNA probes targeting PEDV N gene, and were detected by α-PEDV-N mAb (66-155), α-PEDV-S2 mAb (70-100) and α-PEDV-nsp8 mAb (51-79), respectively. As shown in Figure 3.5.1, at 6 hpi, N, S and Nsp8 can be observed at the perinuclear region. Part of the N protein can be colocalized with viral RNA foci, indicating the RNA binding activity of N protein. The dot-like nsp8 signals are also located in the perinuclear region and can be perfectly co-localized with viral RNA foci, indicating its important role in viral RNA replication and transcriptio. Small amount of S protein was found aggregated in the perinuclear region. Unlike N and nsp8, S protein was not co-localized with RNA foci, indicating that S protein does not associate with the RTC. By 9 hpi, as shown in Figure 3.5.2, a more intense and diffuse labeling pattern was observed in N and S labeled cells. For nsp8, the nsp8-RNA foci can be observed in both perinuclear region and periphery of the cells. By 12 hpi, as shown in Figure 3.5.3, intense and diffuse labeling pattern is still observed in N and S labeled cells, but the amount of Nsp8 is decreased. By 18 hpi, as shown in Figure 3.5.4, the obvious syncytium formation can be

observed. N and S distribute ubiquitously in the multinucleated cells. Nsp8 is still located at the perinuclear region together with the viral RNA foci.

6. Immunohistochemistry

IHC assay was conducted to study the virus infection in the natural host pigs. 7-week-old PEDV negative pigs orally infected with 2 ml homogenized fluid of PEDV positive grounded porcine intestine. On 5 dpi, spleen, lung, tonsil, stomach, mesenteric lymph nodes, duodenum, proximal jejunum, mid jejunum, distal jejunum, cecum, ileum and colon were processed for the assay. PEDV was detected from tissues of mid-jejunum, distal jejunum and ileum, the viral antigens by PEDV mAbs (Figure. 3.6). Coinciding with the positive fluorescence of epithelial cells, infected pigs showed malabsorptive watery diarrhea. From infected intestinal epithelial cells, PEDV N protein was found expressed abundantly, the S2 protein moderately, and the nsp8 protein mildly. Compared to the amount of viral proteins detected in jejunum and ileum, PEDV tended to infect the epithelial cells of jejunum rather than cells of ileum.

Figures

Figure 3.1.1 Prokaryotic expression of PEDV proteins.

SDS-PAGE electrophoresis of recombinant PEDV proteins were expressed in BL21 (DE3), purified, and examind in Coomassie brilliant blue staining. Lanes from left to right, the protein molecular mass standard, PEDV non-structural proteins, nsp1, nsp2 (445-711aa), nsp3 (PLP1), nsp5, nsp7, nsp8, nsp9 and nsp10, and structural proteins S1, S2, M and N.

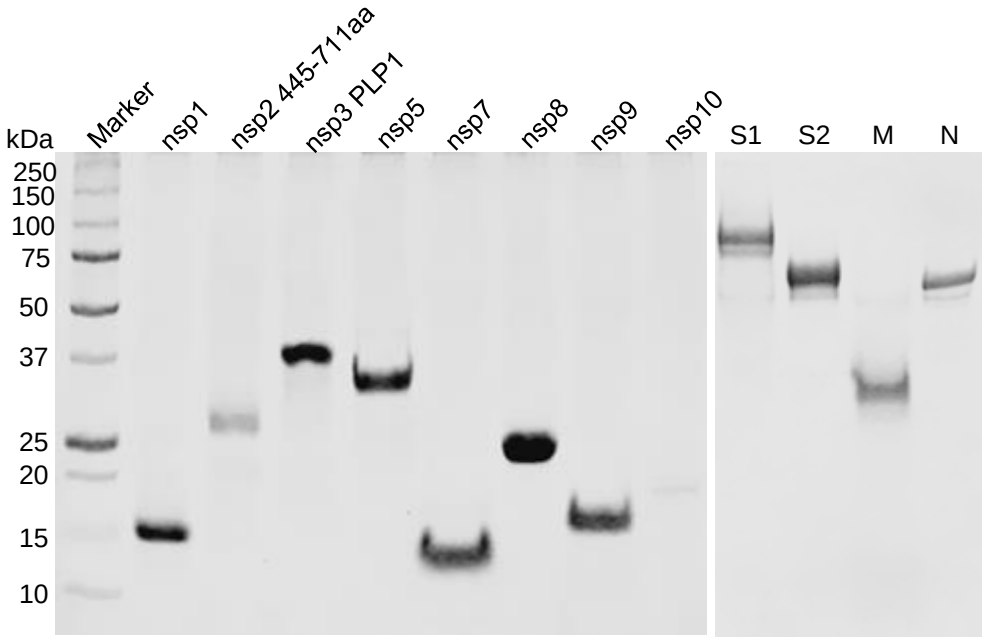

Figure 3.1.2 Western-blot assay result of PEDV proteins detected by porcine PEDV positive serum

In detecting of recombinant proteins with porcine PEDV positive serum by western-blot assay, nsp3 (PLP1), nsp7, nsp8, nsp9, and structural proteins, S1, S2, M and N were recognized. The lanes from left to right were the protein molecular mass standard, PEDV non-structural proteins, including nsp1, nsp2 (445-711aa), nsp3 (PLP1), nsp5, nsp7, nsp8, nsp9 and nsp10, and structural proteins, S1, S2, M and N.

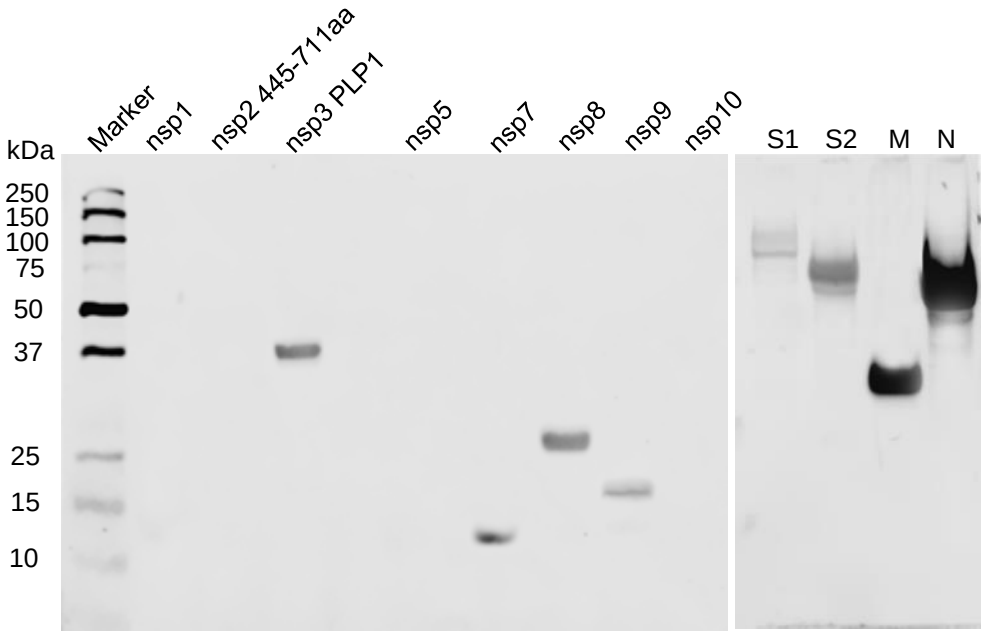

Figure 3.2 ELISA results of PEDV recombinant proteins detected by porcine PEDV positive serum

ELISA was performed to detect the PEDV recombinant proteins by porcine PEDV positive serum. The proteins were ranked based on OD650 values. The Boxes and bars indicated mean OD value and standard deviations.

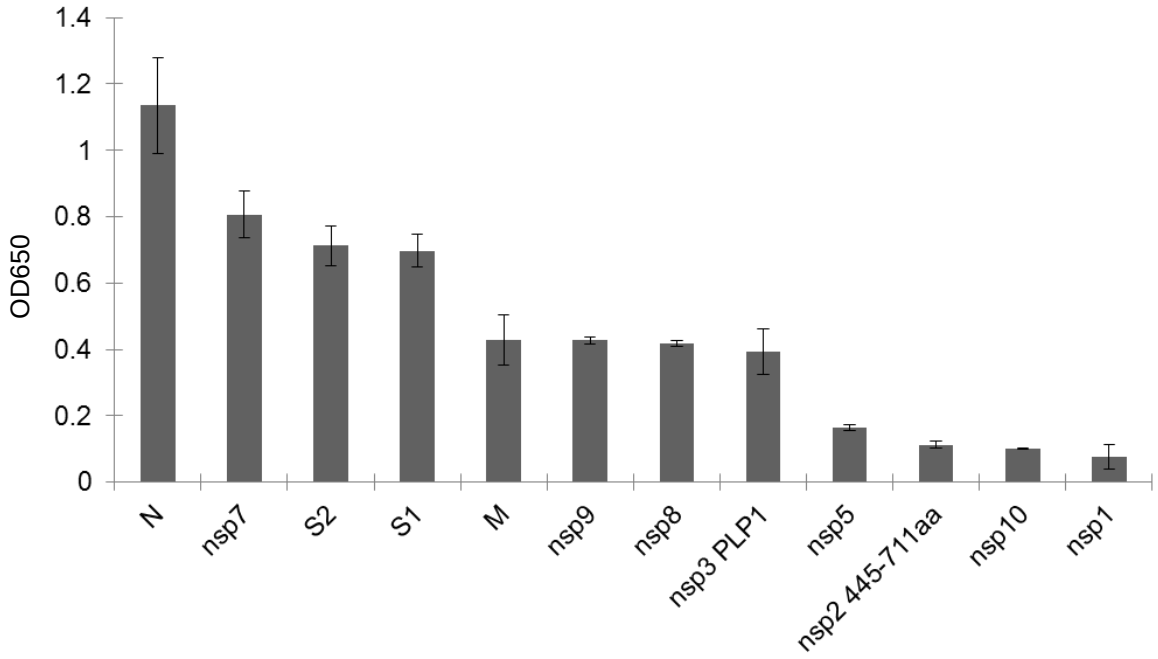

Figure 3.3 epitope mapping

Schematic diagram of the various peptides of PEDV S, N and nsp8 proteins expressed in HEK-293T cells and detected by the mAbs in IFA assay. The red box showed the epitopes of the viral antigen targeted by the mAbs.

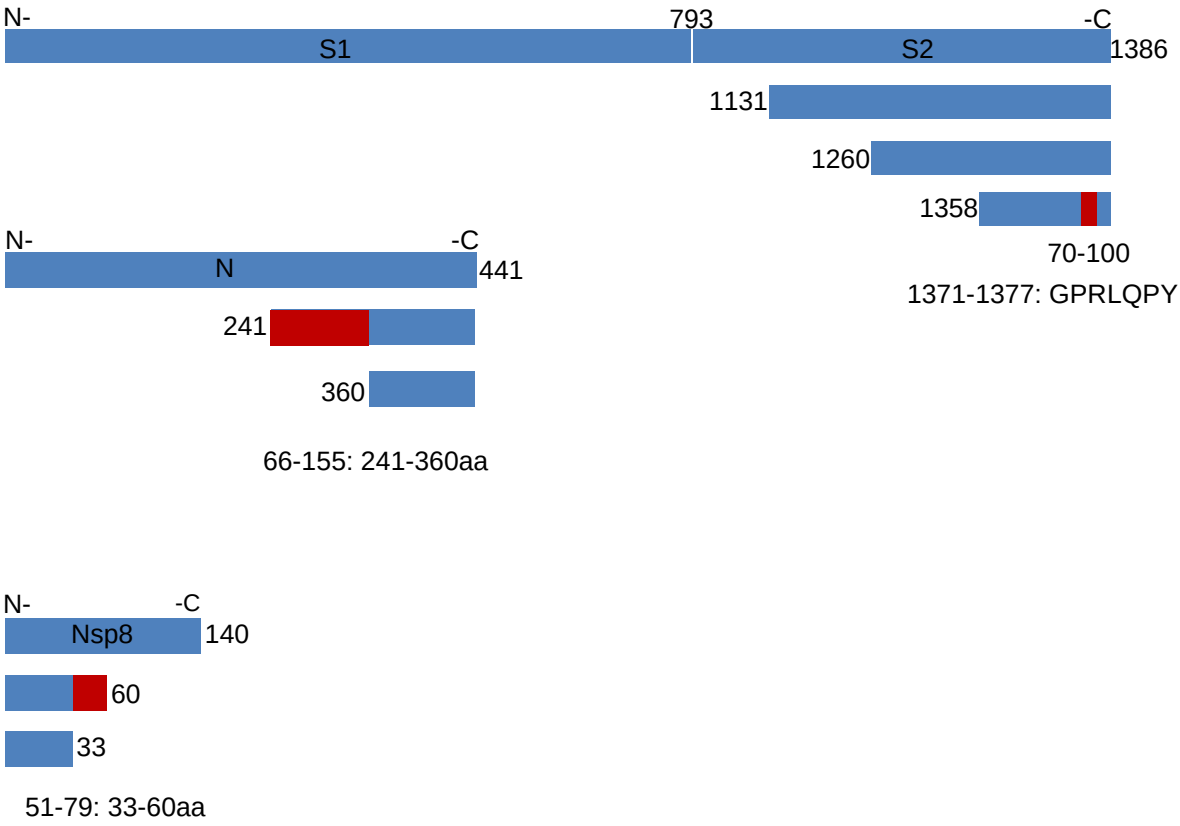

Figure 3.4.1 Immunoprecipitation and Western-blot assay

MAbs against PEDV S (13-519), S2 (70-100), N (66-155) and nsp8 (51-79) tested in immunoprecipitation. Vero76 cells infected with PEDV KS1309 strain (MOI=0.5) and mAbs were employed to pull down the proteins from the cell lysate after 18 hpi. SDS-PAGE electrophoresis (A) and Western-blot assay (B) were done for detection. Recombinant proteins expressed by the pET28α/ BL21 (DE3) were also subjected to the Western-blot assay as control. PEDV +: Vero76 cells infected with PEDV, PEDV -: Mock Vero76 cells, *E. coli* +: PEDV proteins expressed in pET28α/ BL21 (DE3), *E.coli* -: pET28α empty vector expressed in BL21 (DE3). Arrows in red indicate the viral proteins.

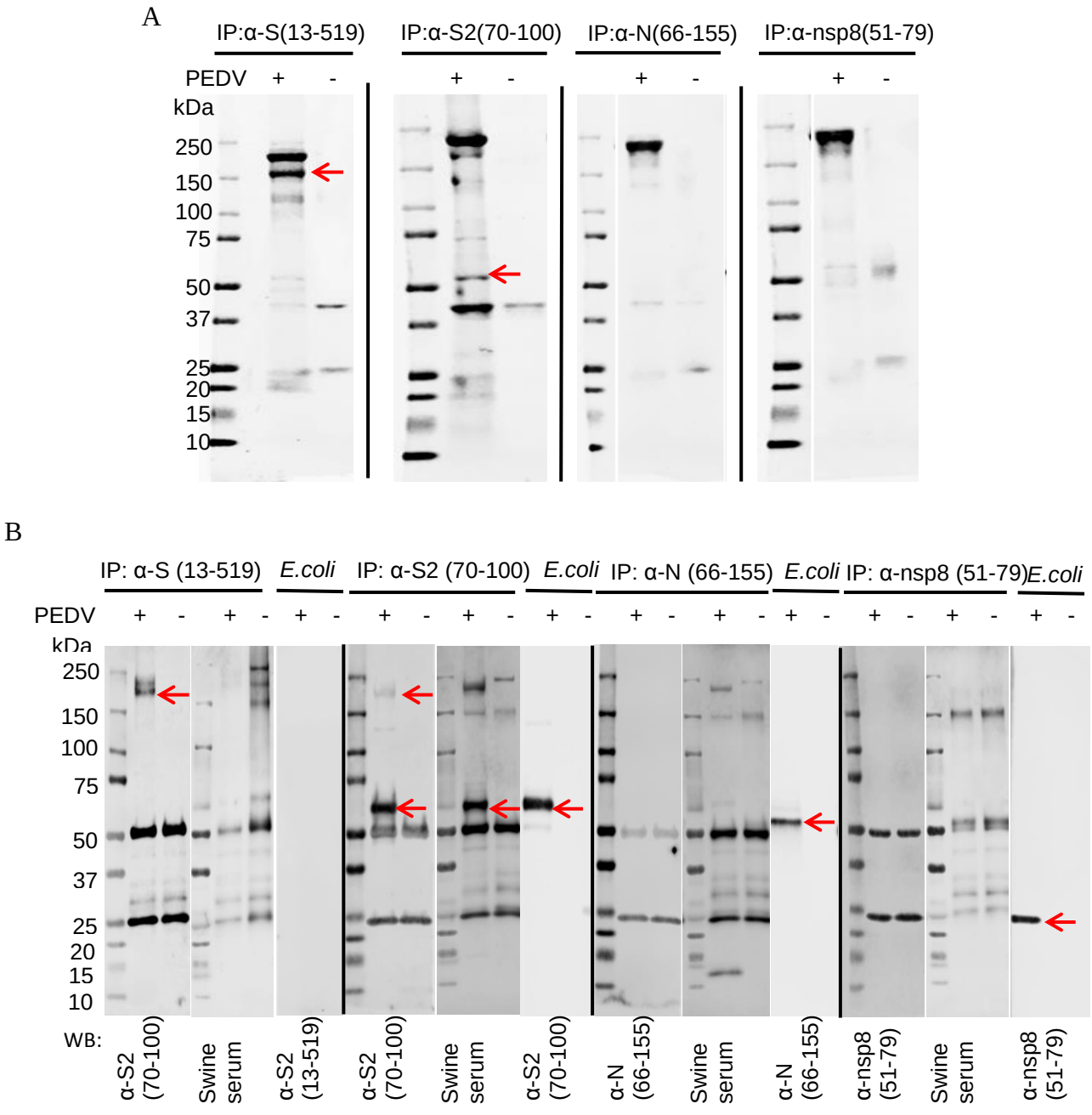

Figure 3.4.2 Identification of cleavage sites in PEDV S protein

PEDV S2 proteins pulled down by mAb 70-100 from the cell lysate. Proteins were separated by SDS-PAGE electrophoresis and transferred to Polyvinylidene difluoride (PVDF) membrane for N terminal peptide sequence (left panel) or to nitrocellulose (NC) membrane for Western-blot assay (right panel). M: Marker, 1: Vero76 cells infected with PEDV, 2: Mock Vero76 cells. Asterisks indicate the S2 proteins.

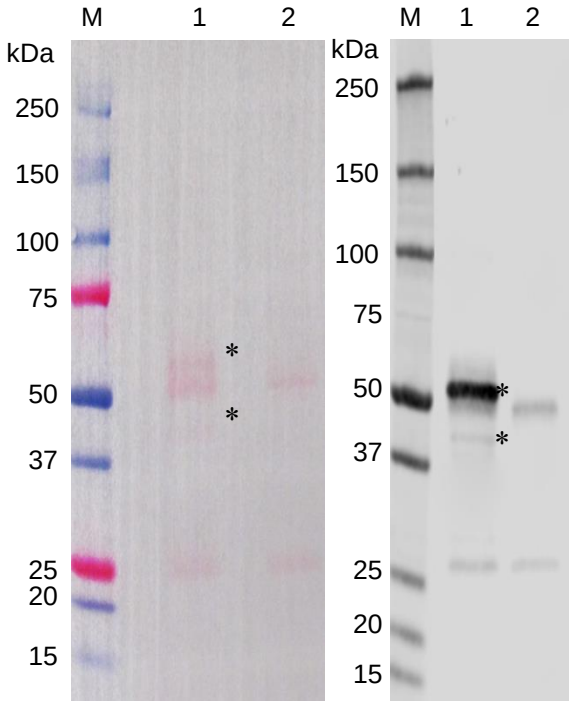

Figure 3.5.1 Intracellular co-localization of S, N and nsp8 with viral genomic RNA at 6 hpi

Vero76 cells infected with PEDV were fixed at 6 hpi, hybridized with the RNA of PEDV N gene Stellaris RNA FISH Probe set labeled with CAL594, and detected by α-PEDV-N mAb (66-155), α-PEDV-S mAb (13-519) and α-PEDV-nsp8 mAb (51-79). Goat-anti-mouse pAb conjugated with ALEXA 488 (Abcam) was used as the secondary antibody. The nucleuses were counterstained with DAPI. Viral protein is in green, RNA in red, and nuclei in blue. Scale bar, 10 μm.

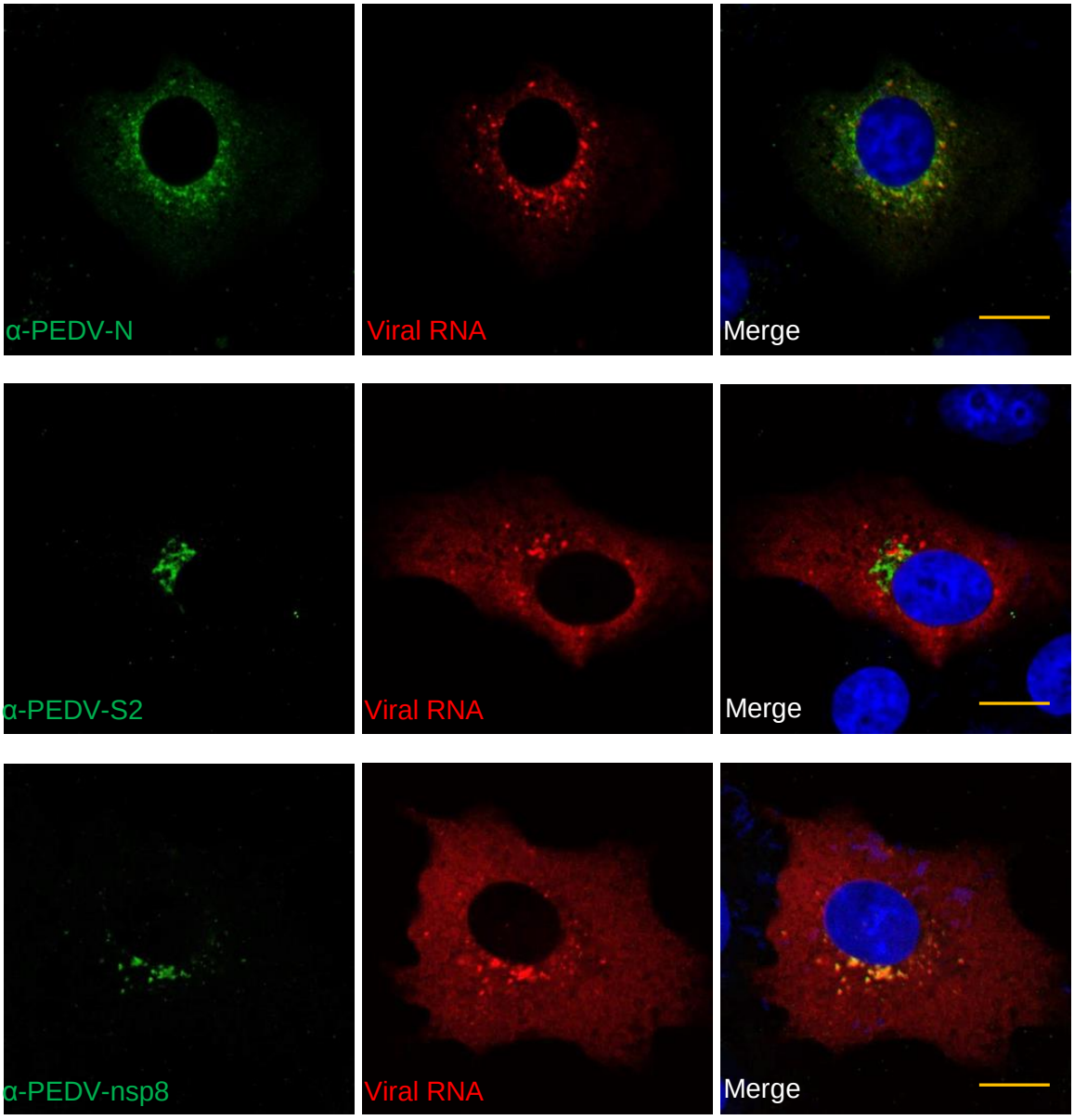

Figure 3.5.2 Intracellular co-localization of S, N and nsp8 with viral genomic RNA at 9 hpi

Vero76 cells infected with PEDV were fixed at 9 hpi, hybridized with the RNA of PEDV N gene Stellaris RNA FISH Probe set labeled with CAL594, and detected by α-PEDV-N mAb (66-155), α-PEDV-S mAb (13-519) and α-PEDV-nsp8 mAb (51-79). Goat-anti-mouse pAb conjugated with ALEXA 488 (Abcam) was used as the secondary antibody. The nucleuses were counterstained with DAPI. Viral protein is in green, RNA in red, and nuclei in blue. Scale bar, 10 μm.

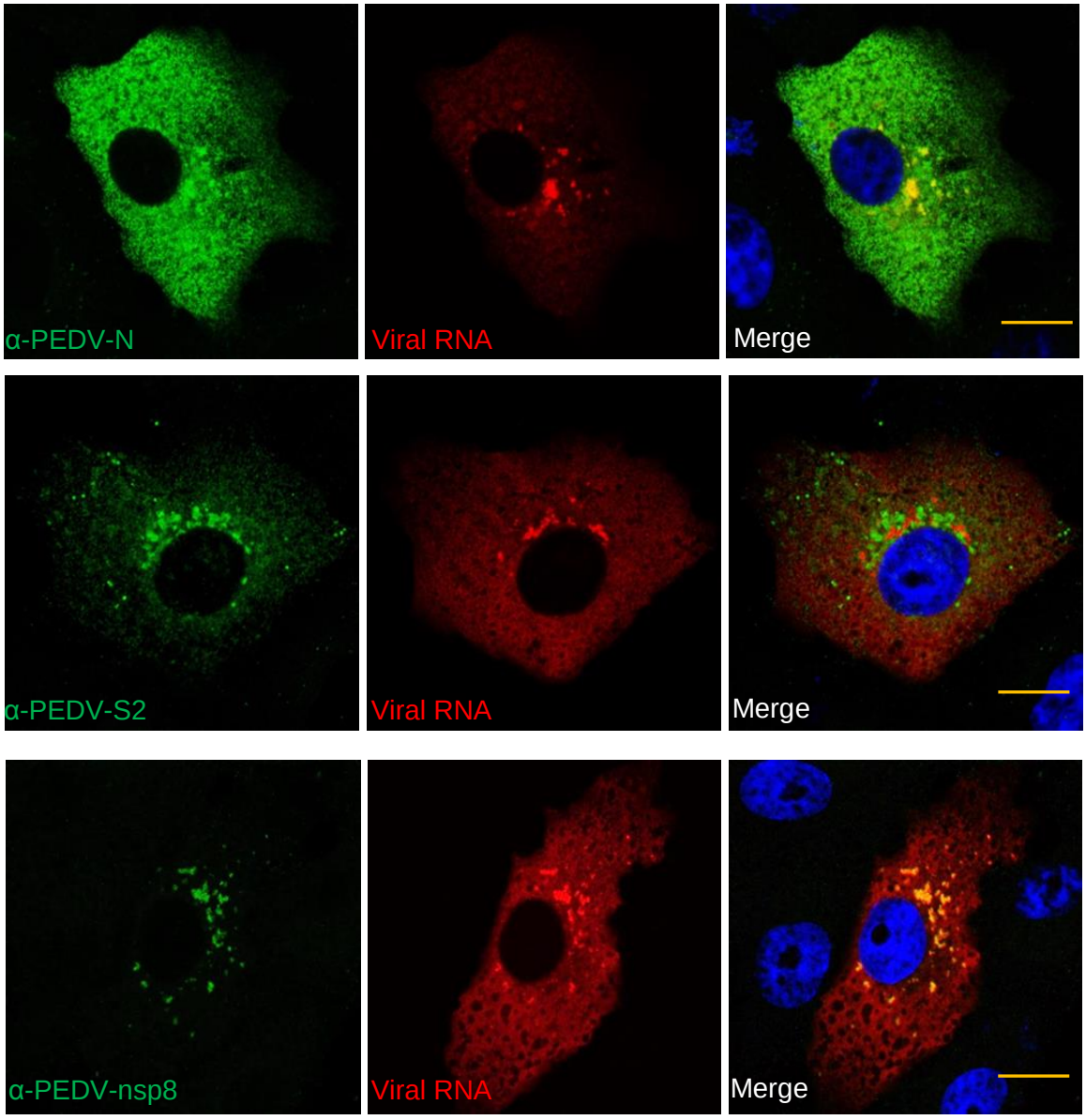

Figure 3.5.3 Intracellular co-localization of S, N and nsp8 with viral genomic RNA at 12 hpi

Vero76 cells infected with PEDV were fixed at 12 hpi, hybridized with the RNA of PEDV N gene Stellaris RNA FISH Probe set labeled with CAL594, and detected by α-PEDV-N mAb (66-155), α-PEDV-S mAb (13-519) and α-PEDV-nsp8 mAb (51-79). Goat-anti-mouse pAb conjugated with ALEXA 488 (Abcam) was used as the secondary antibody. The nucleuses were counterstained with DAPI. Viral protein is in green, RNA in red, and nuclei in blue. Scale bar, 10 μm.

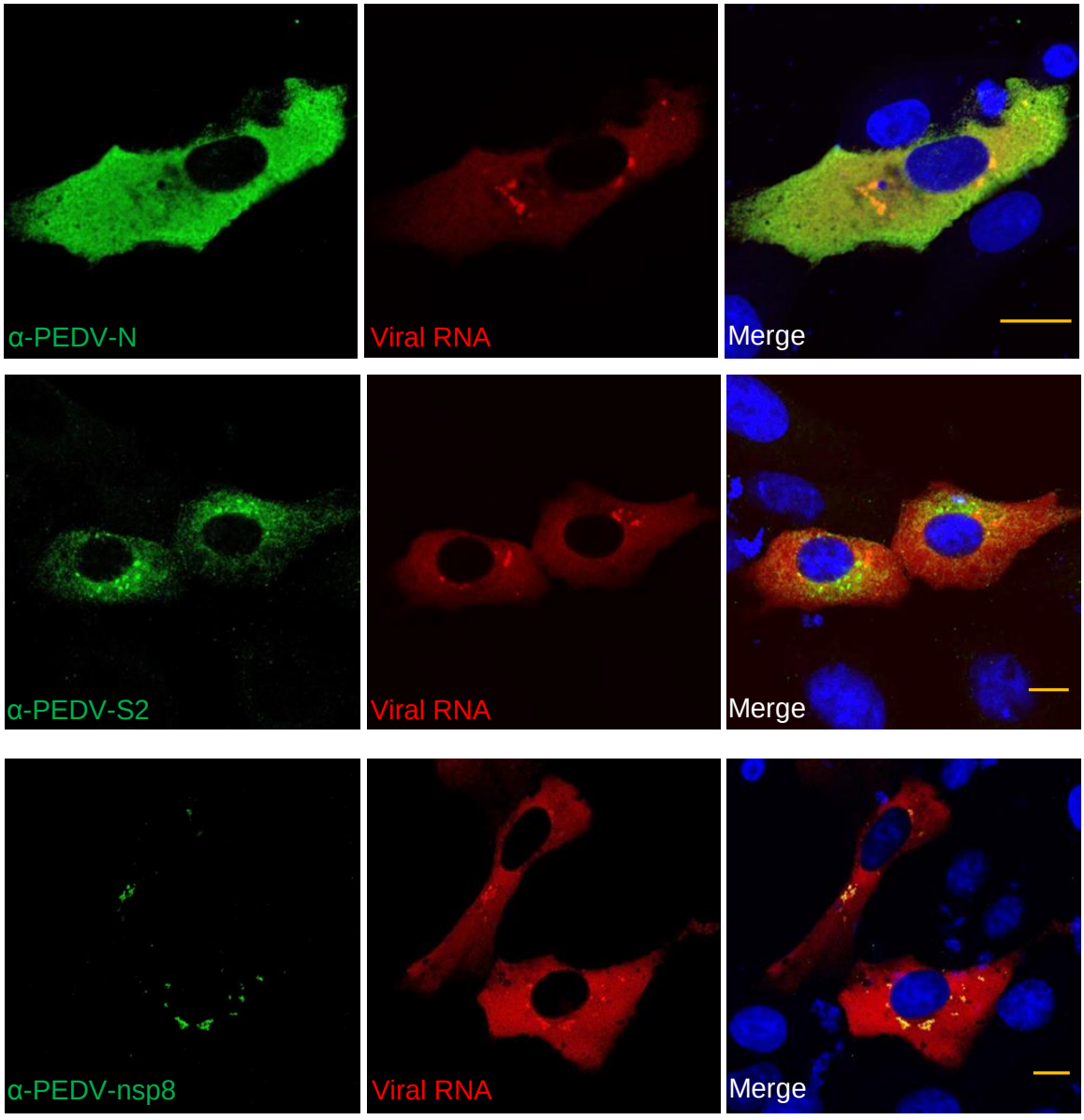

Figure 3.5.4 Intracellular co-localization of S, N and nsp8 with viral genomic RNA at 18 hpi

Vero76 cells infected with PEDV were fixed at 18 hpi, hybridized with the RNA of PEDV N gene Stellaris RNA FISH Probe set labeled with CAL594, and detected by α-PEDV-N mAb (66-155), α-PEDV-S mAb (13-519) and α-PEDV-nsp8 mAb (51-79). Goat-anti-mouse pAb conjugated with ALEXA 488 (Abcam) was used as the secondary antibody. The nucleuses were counterstained with DAPI. Viral protein is in green, RNA in red, and nuclei in blue. Scale bar, 10 μm.

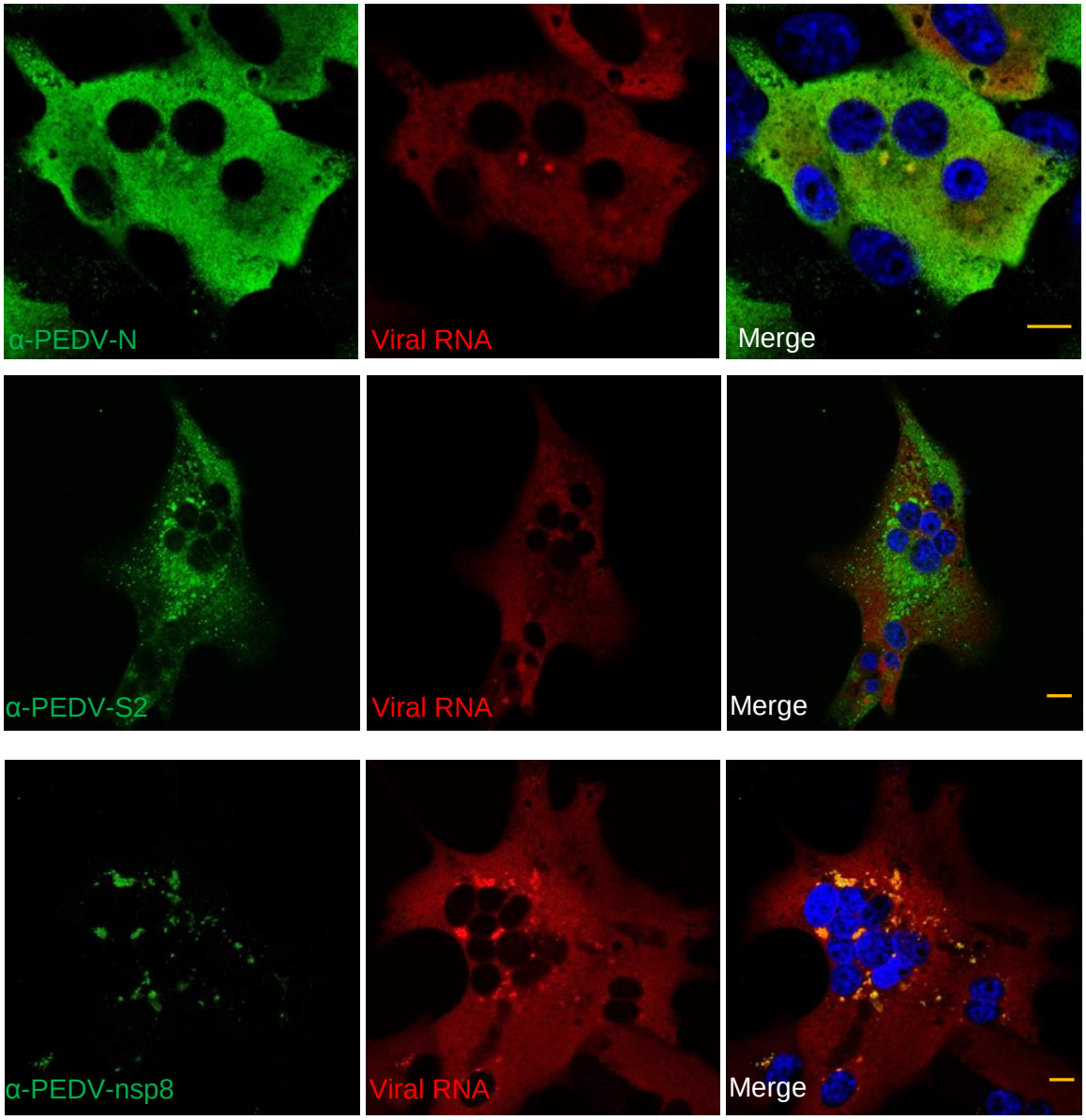

Figure 3.6 Immunohistochemistry (IHC) was conducted on mid-jejunum, distal jejunum and ileum sections.

Immunofluorescent (IF) staining of mid-jejunum, distal jejunum or ileum of a pig at 5 dpi with α-PEDV-N mAb (66-155), α-PEDV-S2 mAb (70-100) and α-PEDV-nsp8 mAb (51-79). Goat-anti-mouse pAb conjugated with ALEXA 488 (Abcam) was used as the secondary antibody. The nucleuses were counterstained with DAPI. The F-actin was stained with ActinRed™ 555 ReadyProbes® Reagent. The results showed the epithelial cells lining atrophied villi were positive for PEDV antigens. Scale bar, 50 μm.

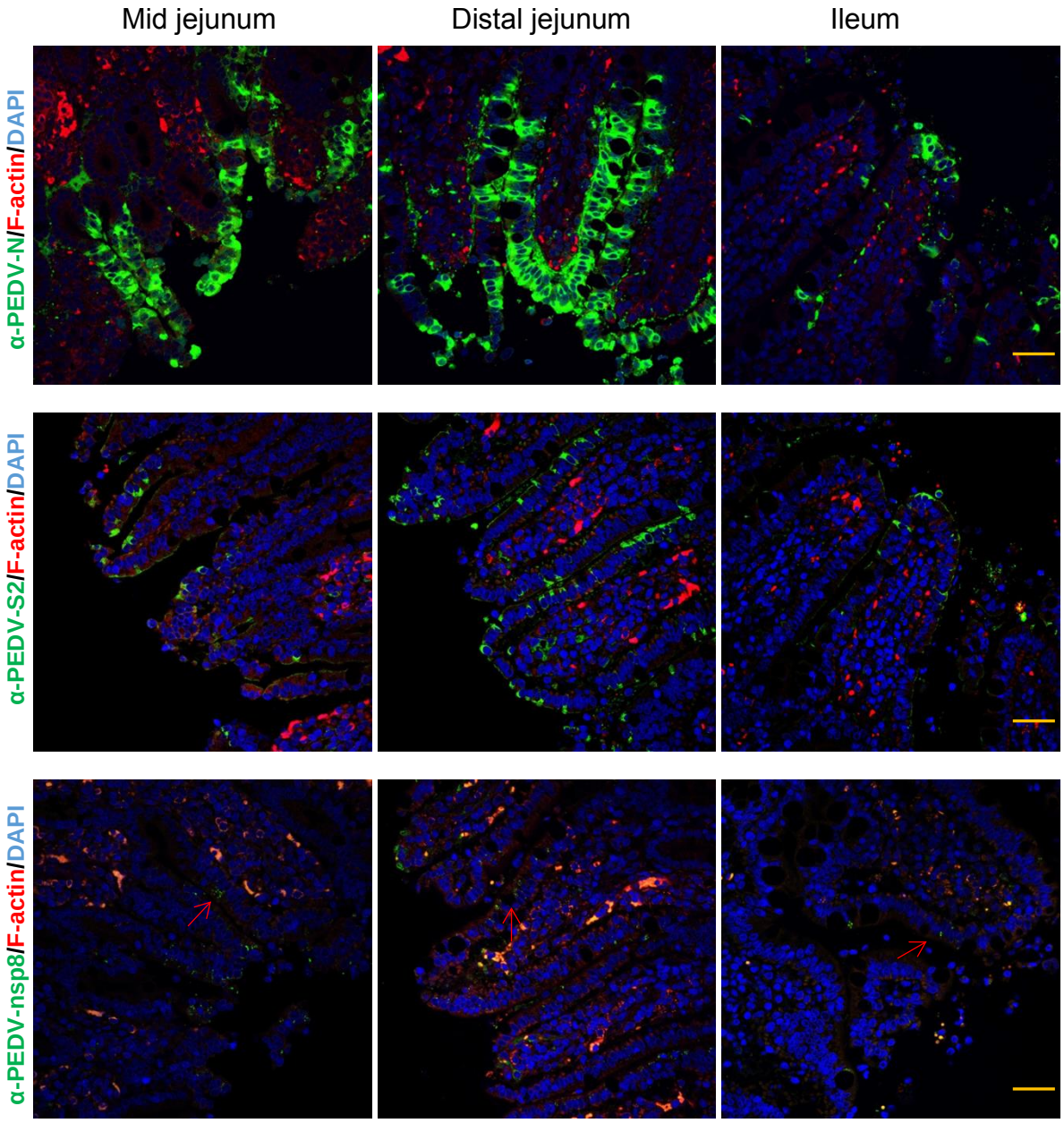

Table 1 Characteristics of PEDV specific mAbs

mAbs	Isotype	Epitope (aa)	Detection assays				
			WB	ELISA	IP	IFA	IHC
13-519	IgG2a	Full-length S*	-	-	+	+	-
70-100	IgG1	1371-1377	S2	+	+	+	+
51-79	IgG1	33-60	Nsp8	+	-	+	+
66-155	IgG1	241-360	N	+	-	+	+

+ : positive; - : negative

*** mAb 13-519 recognizes conformational epitope of S protein**

Table 2 Predicted molecular weight of recombinant proteins in this study

Recombinant Proteins	Predicted Molecular weight (kDa)
nsp1	12.02
Nsp2 (aa 445-711)	26.61
nsp3 (PLP1)	37.43
nsp5	32.79
nsp7	10.99
nsp8	24.05
nsp9	16.91
nsp10	19.09
S1	91.15
S2	70.43
M	28.91
N	54.94

Chapter 4 - Discussion and Conclusion

In this study, recombinant nonstructural and structural PEDV proteins were produced for monoclonal antibody production. Monoclonal antibodies against PEDV S, N and nsp8 proteins were produced and characterized. Results of the Western-blot and ELISA (Fig.3.1.2 & Fig. 3.2), the N, S1, S2, M, nsp7, nsp8 and nsp9 were recognized by the porcine PEDV positive serum. Previous studies demonstrated that the nsp7 and nsp8 formed a hexadecamer to bind genomic RNA and to initiate de novo RNA synthesis as primase and secondary RdRp (34, 35). Therefore, nsp7 and nsp8 were selected to immunize mice for mAbs production and to study the virus replication. The S protein was shown the determinant for the host tropism and virus entry, and standard to assess diversity and relationship among different virus strains. In addition, S protein was found to induce host neutralizing antibody (47, 75). Hence, the S specific mAbs were valuable to study virus pathogenesis. But S protein is a large protein and it is the difficult to express the full lengthed S protein in *E.coli*, we expressed the S1 and S2 separately in this study and mixed the S1 and S2 to immunize mice for the S specific mAb production. Only hybridomas producing mAbs specific for nsp8 and S2 proteins were obtained from the immunized splenocytes, indicating these two proteins were higher antigenic.

All of the four mAbs (13-509, 66-155, 70-100 and 51-79) could be used for the viral detection in vero76 cells infected with PEDV by IFA (Fig. 3.5.1-4). The FISH/ IFA results showed exact colocalization of nsp8 and the viral RNA foci at the perinuclear region at different hpi. N protein was found partially overlapped with viral RNA foci, but S protein appeared no overlapping with the viral RNA foci. In TGEV, nsp8 colocalized with RdRp (nsp12) in the viral factories, which is the main component of the RTC and is responsible for the viral replication and transcription (76). For SARS-CoV, nsp8 together with nsp7 binds to viral RNA not only as

the viral primase, but as the secondary RdRp capable of *de novo* initiation (35, 73). Also, the nsp7 and nsp8 complex of feline coronavirus (FCoV) exhibits primer-indepent RNA polymerase activity (77). Considering the highly conserved activity among coronavirus, it could suggest that RdRp function of PEDV nsp8 supported by the FISH/IFA result here. Coronavirus N protein is known to pack the viral genomic RNA to form the helical nucleocapsid. Of MHV, the N-terminal domain (NTD) of the N protein specifically binds the transcriptional regulatory sequence (TRS) or its complement (cTRS) of the single-stranded RNA (78). In addition, N protein has been demonstrated to associate with the RTC, like N protein of MHV binds to the viral Nsp3 through the NTD and the linker region (LKR) (55, 79). Thus, it is expected that N protein was shown partially colocalized with viral RNA foci. Compared to nsp8 confined at the perinuclear region, N and S protein are dispersed in the whole cytoplasm, participating in the process of viral assembly. In addition, expression level of nsp8 increased at the first 9 hpi, but decreased at 12 hpi, which was similar to the activity of SARS-CoV RTC, peaked at 6 hpi, but diminished significantly in the late post-infection stages (74).

The mAbs 70-100, 66-155 and 51-79 recognizing linear epitopes detected recombinant S2, N, and nsp8 proteins respectively. But the conformational mAb 13-519 did not detect S2, N or nsp8 (Fig.3.4.1). However, the IP analysis showed that the mAbs 13-519 and 70-100 interacted strongly with the naïve spike protein from the virus infected cell lysate. Interestingly, along with a putative band of S2 protein at 50-75 kDa (80), another band migrates at the site 37 to 50 kDa was also pulled down and detected by mAb 70-100 (Fig.3.4.2). This samller band was sequenced at N-terminal, and the sequence showed that a cleavage site existed at R890. A previous study predicted this S2' site and demonstrated the importance of this site during PEDV

entry and synsytial formation (49). Our study confirmed this S2' site and detected the cleaved products S2' in the PEDV infected cells.

The IHC is a powerful diagnostic tool for both human and animal diseases. In this study, mAbs 66-155, 70-100 and 51-79 successfully detected the viral antigens in the villous epithelial cells of mid-jejunum, distal jejunum and ileum. That is consistent with other studies indicating jejunum and ileum are the primary sites of PEDV infection (12) (Fig.3.6). The mAb 66-155 (anti-PEDV N) was showed strong fluorescence signal, indicating this antibody can be further used for IHC diagnostic assay development. The mAb 13-519 (anti-PEDV S) was unable to detect the viral antigens in the tissue. That is probably caused by the great difference in S amino acid sequence between KS1309 strain and the field PEDV strain used in this study, as previous study demonstrated that coronavirus Spike protein has relatively higher mutation rate to evade the host immune surveillance (81). However, it could also result from the possibility that the conformational epitope of spike protein may be destroyed during sample preparation of the IHC test.

In conclusion, four mAbs specific for PEDV N, S, S2 and nsp8 proteins, respectively, were produced and characterized by various biological assays, including indirect IFA, ELISA, Western Blot, IP, IHC test and FISH. Results indicated this panel of mAbs valuable tools for PEDV diagnostics and pathogenesis studies.

Reference

1. Stevenson GW, *et al.* (2013) Emergence of Porcine epidemic diarrhea virus in the United States: clinical signs, lesions, and viral genomic sequences. *J Vet Diagn Invest* 25(5):649-654.
2. E.N. W (1977) An apparently new syndrome of porcine epidemic diarrhea. *Vet Rec* 100:243-410.
3. Pensaert MB & de Bouck P (1978) A new coronavirus-like particle associated with diarrhea in swine. *Arch Virol* 58(3):243-247.
4. Chasey D & Cartwright SF (1978) Virus-Like Particles Associated with Porcine Epidemic Diarrhea. *Res Vet Sci* 25(2):255-256.
5. Sm íd B. VL, Rod ák L., Kudrna J., Musilov á J. (1993) The causal agent was demonstrated in intestinal contents by EM and identified by immune EM. *Vet Med (Praha)* 38(6):333-341.
6. Takahashi K, Okada K, & Ohshima K (1983) An Outbreak of Swine Diarrhea of a New-Type Associated with Coronavirus-Like Particles in Japan. *Jpn J Vet Sci* 45(6):829-832.
7. Kweon CH, Kwon, B.J., Jung, T.S., Kee, Y.J., Hur, D.H., Hwang, E.K., Rhee, J.C., An, S.H. (1993) Isolation of porcine epidemic diarrhea virus (PEDV) infection in Korea. *Korean Journal of Veterinary Research* 33(259-254).
8. Sun RQ, *et al.* (2012) Outbreak of Porcine Epidemic Diarrhea in Suckling Piglets, China. *Emerg Infect Dis* 18(1):161-163.
9. Jinghui F & Yijing L (2005) Cloning and sequence analysis of the M gene of porcine epidemic diarrhea virus LJB/03. *Virus Genes* 30(1):69-73.
10. Duy D.T. TNT, Puranaveja S., Thanawongnuwech R. (2011) Genetic Characterization of Porcine Epidemic Diarrhea Virus (PEDV) Isolates from Southern Vietnam during 2009–2010 Outbreaks. *Thai J Vet Med* 41:55-64.
11. Puranaveja S, *et al.* (2009) Chinese-like Strain of Porcine Epidemic Diarrhea Virus, Thailand. *Emerg Infect Dis* 15(7):1112-1115.
12. Jung K & Saif LJ (2015) Porcine epidemic diarrhea virus infection: Etiology, epidemiology, pathogenesis and immunoprophylaxis. *Vet J* 204(2):134-143.
13. Liu C, *et al.* (2015) Receptor Usage and Cell Entry of Porcine Epidemic Diarrhea Coronavirus. *J Virol* 89(11):6121-6125.
14. Hofmann M & Wyler R (1988) Propagation of the Virus of Porcine Epidemic Diarrhea in Cell-Culture. *J Clin Microbiol* 26(11):2235-2239.
15. Kamau NA, *et al.* (2010) Susceptibility of Mice to Porcine Epidemic Diarrhea Virus. *J Anim Vet Adv* 9(24):3114-3116.
16. Wang S, *et al.* (2014) Classification of emergent U.S. strains of porcine epidemic diarrhea virus by phylogenetic analysis of nucleocapsid and ORF3 genes. *J Clin Microbiol* 52(9):3509-3510.
17. Oka T, *et al.* (2014) Cell culture isolation and sequence analysis of genetically diverse US porcine epidemic diarrhea virus strains including a novel strain with a large deletion in the spike gene. *Vet Microbiol* 173(3-4):258-269.
18. Perlman S & Netland J (2009) Coronaviruses post-SARS: update on replication and pathogenesis. *Nat Rev Microbiol* 7(6):439-450.

19. Du LY, *et al.* (2009) The spike protein of SARS-CoV - a target for vaccine and therapeutic development. *Nat Rev Microbiol* 7(3):226-236.
20. Ziebuhr J (2005) The coronavirus replicase. *Curr Top Microbiol* 287:57-94.
21. Jansson AM (2013) Structure of Alphacoronavirus Transmissible Gastroenteritis Virus nsp1 Has Implications for Coronavirus nsp1 Function and Evolution. *J Virol* 87(5):2949-2955.
22. Almeida MS, Johnson MA, Herrmann T, Geralt M, & Wuthrich K (2007) Novel beta-barrel fold in the nuclear magnetic resonance structure of the replicase nonstructural protein 1 from the severe acute respiratory syndrome coronavirus. *J Virol* 81(7):3151-3161.
23. Huang C. LKG, Rozovics J.M., Narayanan K., Semler B.L., Makino S. (2011) Alphacoronavirus transmissible gastroenteritis virus nsp1 protein suppresses protein translation in mammalian cells and in cell-free HeLa cell extracts but not in rabbit reticulocyte lysate. . *J Virol* 85:638–643.
24. Kamitani W. HC, Narayanan K., Lokugamage K.G., Makino S. (2009) A novel two-pronged strategy to suppress host protein synthesis by SARS coronavirus nsp1 protein. *Nat. Struct. Mol. Biol.* 16:1134-1140.
25. Graham RL, Sims AC, Brockway SM, Baric RS, & Denison MR (2005) The nsp2 replicase proteins of murine hepatitis virus and severe acute respiratory syndrome coronavirus are dispensable for viral replication. *J Virol* 79(21):13399-13411.
26. Ziebuhr J, Snijder EJ, & Gorbalenya AE (2000) Virus-encoded proteinases and proteolytic processing in the Nidovirales. *J Gen Virol* 81:853-879.
27. Han YS, *et al.* (2005) Papain-like protease 2 (PLP2) from severe acute respiratory syndrome coronavirus (SARS-CoV): Expression, purification, characterization, and inhibition. *Biochemistry-Us* 44(30):10349-10359.
28. Clementz MA, *et al.* (2010) Deubiquitinating and Interferon Antagonism Activities of Coronavirus Papain-Like Proteases. *J Virol* 84(9):4619-4629.
29. Xu YY, *et al.* (2009) Crystal Structures of Two Coronavirus ADP-Ribose-1 "-Monophosphatases and Their Complexes with ADP-Ribose: a Systematic Structural Analysis of the Viral ADRP Domain. *J Virol* 83(2):1083-1092.
30. Serrano P, *et al.* (2009) Nuclear Magnetic Resonance Structure of the Nucleic Acid-Binding Domain of Severe Acute Respiratory Syndrome Coronavirus Nonstructural Protein 3. *J Virol* 83(24):12998-13008.
31. Clementz MA, Kanjanahaluethai A, O'Brien TE, & Baker SC (2008) Mutation in murine coronavirus replication protein nsp4 alters assembly of double membrane vesicles. *Virology* 375(1):118-129.
32. Deming DJ, Graham RL, Denison MR, & Baric RS (2007) Processing of open reading frame 1a replicase proteins nsp7 to nsp10 in murine hepatitis virus strain A59 replication. *J Virol* 81(19):10280-10291.
33. Knoops K, *et al.* (2008) SARS-coronavirus replication is supported by a reticulovesicular network of modified endoplasmic reticulum. *Plos Biol* 6(9):1957-1974.
34. Zhai YJ, *et al.* (2005) Insights into SARS-CoV transcription and replication from the structure of the nsp7-nsp8 hexadecamer. *Nat Struct Mol Biol* 12(11):980-986.
35. Velthuis AJWT, van den Worm SHE, & Snijder EJ (2012) The SARS-coronavirus nsp7+nsp8 complex is a unique multimeric RNA polymerase capable of both de novo initiation and primer extension. *Nucleic Acids Res* 40(4):1737-1747.

36. Egloff MP, *et al.* (2004) The severe acute respiratory syndrome-coronavirus replicative protein nsp9 is a single-stranded RNA-binding subunit unique in the RNA virus world. *P Natl Acad Sci USA* 101(11):3792-3796.
37. Miknis ZJ, *et al.* (2009) Severe Acute Respiratory Syndrome Coronavirus nsp9 Dimerization Is Essential for Efficient Viral Growth. *J Virol* 83(7):3007-3018.
38. Bouvet M, *et al.* (2014) Coronavirus Nsp10, a Critical Co-factor for Activation of Multiple Replicative Enzymes. *J Biol Chem* 289(37):25783-25796.
39. Su D, *et al.* (2006) Dodecamer structure of severe acute respiratory syndrome coronavirus nonstructural protein nsp10. *J Virol* 80(16):7902-7908.
40. Chen Y, *et al.* (2009) Functional screen reveals SARS coronavirus nonstructural protein nsp14 as a novel cap N7 methyltransferase. *P Natl Acad Sci USA* 106(9):3484-3489.
41. Decroly E, *et al.* (2011) Crystal Structure and Functional Analysis of the SARS-Coronavirus RNA Cap 2 '-O-Methyltransferase nsp10/nsp16 Complex. *Plos Pathog* 7(5).
42. Eckerle LD, Lu X, Sperry SM, Choi L, & Denison MR (2007) High fidelity of murine hepatitis virus replication is decreased in nsp14 exoribonuclease mutants. *J Virol* 81(22):12135-12144.
43. Fang SG, Shen HY, Wang JB, Tay FPL, & Liu DX (2008) Proteolytic processing of polyproteins 1a and 1ab between non-structural proteins 10 and 11/12 of Coronavirus infectious bronchitis virus is dispensable for viral replication in cultured cells. *Virology* 379(2):175-180.
44. Velthuis AJWT, Arnold JJ, Cameron CE, van den Worm SHE, & Snijder EJ (2011) The RNA polymerase activity of SARS-coronavirus nsp12 is primer dependent (vol 38, pg 203, 2010). *Nucleic Acids Res* 39(21):9458-9458.
45. Ivanov KA, *et al.* (2004) Major genetic marker of nidoviruses encodes a replicative endoribonuclease. *P Natl Acad Sci USA* 101(34):12694-12699.
46. Bosch BJ, Bartelink W, & Rottier PJM (2008) Cathepsin L functionally cleaves the severe acute respiratory syndrome coronavirus class I fusion protein upstream of rather than adjacent to the fusion peptide. *J Virol* 82(17):8887-8890.
47. Li WH, *et al.* (2005) Receptor and viral determinants of SARS-coronavirus adaptation to human ACE2. *Embo J* 24(8):1634-1643.
48. Belouzard S, Chu VC, & Whittaker GR (2009) Activation of the SARS coronavirus spike protein via sequential proteolytic cleavage at two distinct sites. *P Natl Acad Sci USA* 106(14):5871-5876.
49. Wicht O, *et al.* (2014) Identification and Characterization of a Proteolytically Primed Form of the Murine Coronavirus Spike Proteins after Fusion with the Target Cell. *J Virol* 88(9):4943-4952.
50. Wicht O, *et al.* (2014) Proteolytic activation of the porcine epidemic diarrhea coronavirus spike fusion protein by trypsin in cell culture. *J Virol* 88(14):7952-7961.
51. Hsieh PK, *et al.* (2005) Assembly of severe acute respiratory syndrome coronavirus RNA packaging signal into virus-like particles is nucleocapsid dependent. *J Virol* 79(22):13848-13855.
52. Chang CK, *et al.* (2006) Modular organization of SARS coronavirus nucleocapsid protein. *J Biomed Sci* 13(1):59-72.
53. Chang CK, *et al.* (2009) Multiple Nucleic Acid Binding Sites and Intrinsic Disorder of Severe Acute Respiratory Syndrome Coronavirus Nucleocapsid Protein: Implications for Ribonucleocapsid Protein Packaging. *J Virol* 83(5):2255-2264.

54. Huang QL, *et al.* (2004) Structure of the N-terminal RNA-binding domain of the SARS CoV nucleocapsid protein. *Biochemistry-Us* 43(20):6059-6063.
55. Keane SC & Giedroc DP (2013) Solution Structure of Mouse Hepatitis Virus (MHV) nsp3a and Determinants of the Interaction with MHV Nucleocapsid (N) Protein. *J Virol* 87(6):3502-3515.
56. Kopecky-Bromberg SA, Martinez-Sobrido L, Frieman M, Baric RA, & Palese P (2007) Severe acute respiratory syndrome coronavirus open reading frame (ORF) 3b, ORF 6, and nucleocapsid proteins function as interferon antagonists. *J Virol* 81(2):548-557.
57. Ding Z, *et al.* (2014) Porcine Epidemic Diarrhea Virus Nucleocapsid Protein Antagonizes Beta Interferon Production by Sequestering the Interaction between IRF3 and TBK1. *J Virol* 88(16):8936-8945.
58. Arndt AL, Larson BJ, & Hogue BG (2010) A Conserved Domain in the Coronavirus Membrane Protein Tail Is Important for Virus Assembly. *J Virol* 84(21):11418-11428.
59. Fischer F, Stegen CF, Masters PS, & Samsonoff WA (1998) Analysis of constructed E gene mutants of mouse hepatitis virus confirms a pivotal role for E protein in coronavirus assembly. *J Virol* 72(10):7885-7894.
60. Snijder EJ, *et al.* (2006) Ultrastructure and origin of membrane vesicles associated with the severe acute respiratory syndrome coronavirus replication complex. *J Virol* 80(12):5927-5940.
61. Angelini MM, Akhlaghpour M, Neuman BW, & Buchmeier MJ (2013) Severe Acute Respiratory Syndrome Coronavirus Nonstructural Proteins 3, 4, and 6 Induce Double-Membrane Vesicles. *Mbio* 4(4).
62. Pospischil A, Stuedli A, & Kiupel M (2002) Update on porcine epidemic diarrhea. *J Swine Health Prod* 10(2):81-85.
63. Li BX, Ge JW, & Li YJ (2007) Porcine aminopeptidase N is a functional receptor for the PEDV coronavirus. *Virology* 365(1):166-172.
64. Madson DM, *et al.* (2014) Pathogenesis of porcine epidemic diarrhea virus isolate (US/Iowa/18984/2013) in 3-week-old weaned pigs. *Vet Microbiol* 174(1-2):60-68.
65. Mooseker MS (1985) Organization, Chemistry, and Assembly of the Cytoskeletal Apparatus of the Intestinal Brush-Border. *Annu Rev Cell Biol* 1:209-241.
66. Ducatelle R, Coussement W, Debouck P, & Hoorens J (1982) Pathology of experimental CV777 coronavirus enteritis in piglets. II. Electron microscopic study. *Vet Pathol* 19(1):57-66.
67. Kim YS & Ho SB (2010) Intestinal goblet cells and mucins in health and disease: recent insights and progress. *Curr Gastroenterol Rep* 12(5):319-330.
68. Stevenson GW & Fox MA (2013) The neuropharmacology of the age-old sedative/hypnotic, ethanol. *Front Neurosci* 7:122.
69. Song D & Park B (2012) Porcine epidemic diarrhoea virus: a comprehensive review of molecular epidemiology, diagnosis, and vaccines. *Virus Genes* 44(2):167-175.
70. Johnson CR, Yu WQ, & Murtaugh MP (2007) Cross-reactive antibody responses to nsp1 and nsp2 of Porcine reproductive and respiratory syndrome virus. *J Gen Virol* 88:1184-1195.
71. Fang Y, Pekosz A, Haynes L, Nelson EA, & Rowland RRR (2006) Production and characterization of monoclonal antibodies against the nucleocapsid protein of SARS-CoV. *Adv Exp Med Biol* 581:153-156.

72. Cruz DJM, Kim CJ, & Shin HJ (2006) Phage-displayed peptides having antigenic similarities with porcine epidemic diarrhea virus (PEDV) neutralizing epitopes. *Virology* 354(1):28-34.
73. Imbert I, *et al.* (2006) A second, non-canonical RNA-dependent RNA polymerase in SARS coronavirus. *Embo J* 25(20):4933-4942.
74. Li S, *et al.* (2010) New nsp8 isoform suggests mechanism for tuning viral RNA synthesis. *Protein Cell* 1(2):198-204.
75. Qi Chen GL, Judith Stasko, Joseph T. Thomas, Wendy R. Stensland, Angela E. Pillatzki, Phillip C. Gauger, Kent J. Schwartz, Darin Madson, Kyoung-Jin Yoon, Gregory W. Stevenson, Eric R. Burrough, Karen M. Harmon, Rodger G. Main and Jianqiang Zhang (2014) Isolation and Characterization of Porcine Epidemic Diarrhea Viruses Associated with the 2013 Disease Outbreak in US Swine. *J Clin Microbiol.* 52(1):234-243.
76. Nogales A, Marquez-Jurado S, Galan C, Enjuanes L, & Almazan F (2012) Transmissible Gastroenteritis Coronavirus RNA-Dependent RNA Polymerase and Nonstructural Proteins 2, 3, and 8 Are Incorporated into Viral Particles. *J Virol* 86(2):1261-1266.
77. Xiao YB, *et al.* (2012) Nonstructural Proteins 7 and 8 of Feline Coronavirus Form a 2:1 Heterotrimer That Exhibits Primer-Independent RNA Polymerase Activity. *J Virol* 86(8):4444-4454.
78. Grossoehme NE, *et al.* (2009) Coronavirus N Protein N-Terminal Domain (NTD) Specifically Binds the Transcriptional Regulatory Sequence (TRS) and Melts TRS-cTRS RNA Duplexes. *J Mol Biol* 394(3):544-557.
79. Verheije MH, *et al.* (2010) The Coronavirus Nucleocapsid Protein Is Dynamically Associated with the Replication-Transcription Complexes. *J Virol* 84(21):11575-11579.
80. Huang YW, *et al.* (2013) Origin, Evolution, and Genotyping of Emergent Porcine Epidemic Diarrhea Virus Strains in the United States. *Mbio* 4(5).
81. Vlasova A.N. MD, Wang Q., Culhane M. R., Rossow K., Rovira A., Collins J., and Jung K. (2014) Distinct Characteristics and Complex Evolution of PEDV Strains, North America, May 2013–February. *Emerg Infect Dis* 20(10):1620-1628.